easyCLIP Quantifies RNA-Protein Interactions and Characterizes Recurrent PCBP1 Mutations in Cancer

Authors: Douglas F. Porter[1], Paul A. Khavari[1]*

Affiliations:

[1]Program in Epithelial Biology, Stanford University, Stanford, CA 94305 and the Stanford Program in Cancer Biology, Stanford University, Stanford, CA 94305

*Correspondence to: khavari@stanford.edu

ABSTRACT

RNA-protein interactions mediate a host of cellular processes, underscoring the need for methods to quantify their occurrence in living cells. RNA interaction frequencies for the average cellular protein are undefined, however, and there is no quantitative threshold to define a protein as an RNA-binding protein (RBP). Ultraviolet (UV) cross-linking immunoprecipitation (CLIP)-sequencing, an effective and widely used means of characterizing RNA-protein interactions, would particularly benefit from the capacity to quantitate the number of RNA cross-links per protein per cell. In addition, CLIP-seq methods are difficult, have high experimental failure rates and many ambiguous analytical decisions. To address these issues, the easyCLIP method was developed and used to quantify RNA-protein interactions for a panel of known RBPs as well as a spectrum of random non-RBP proteins. easyCLIP provides the advantages of good efficiency compared to current standards, a simple protocol with a very low failure rate, troubleshooting information that includes direct visualization of prepared libraries without amplification, and a new form of analysis. easyCLIP, which uses sequential on-bead ligation of 5' and 3' adapters tagged with different infrared dyes, classified non-RBPs as those with a per protein RNA cross-link rate of <0.1%, with most RBPs substantially above this threshold, including Rbfox1 (18%), hnRNPC (22%), CELF1 (11%), FBL (2%), and STAU1 (1%). easyCLIP with the PCBP1^{L100} RBP mutant recurrently seen in cancer quantified increased RNA binding compared to wild-type PCBP1 and suggested a potential mechanism for this RBP mutant in cancer. easyCLIP provides a simple, efficient and robust method to both obtain both traditional CLIP-seq information and to define actual RNA interaction frequencies for a given protein, enabling quantitative cross-RBP comparisons as well as insight into RBP mechanisms.

63 ***Introduction***
64 The number of RNA-protein interaction datasets is growing rapidly, raising the importance of
65 being able to integrate them into models of the global RNA-protein interactome and the
66 challenges of integrating such data between RNA-binding proteins (RBPs) was recently
67 highlighted[1]. The physical reality of RNA-protein interactions is their individual occurrence in
68 individual cells, which may be abstracted to an average complex number per-cell in a
69 population. The RNA-protein complex count per-cell may be normalized to derive the number
70 of complexes per-interaction partner. It is these frequencies, per-cell and per-interaction
71 partner, that are the most basic characterizations of RNA-protein interaction networks.
72 Determining the targets of an RBP by enrichment over negative control immunopurifications,
73 or by clustering of cross-links, or many such other approaches, are all ultimately inferring that
74 the absolute count of an RNA-protein complex in the cell is abnormally high. The estimation
75 of per-cell and per-protein absolute quantities provide the ultimate framework for describing
76 a global and widely reproducible view of RNA-protein interactions.
77
78 There is currently no general method to estimate absolute RNA-protein interaction
79 frequencies, either by cross-linking or by other means. Relative interaction frequencies have
80 been estimated by comparing co-purified radiolabeled RNA, but this method does not yield
81 absolute numbers. It is possible to estimate cross-link rates by observing the amount of UV-
82 and RNAse-dependent decrease in an immunoblot blot band for proteins that cross-link well,
83 but this is not feasible for proteins with a cross-link rate of ~1%. Western blot quantification
84 is further complicated by the fact that absolute quantification requires protein in single bands
85 of at least 5 ng, the narrow region of linear signal in immunoblots, and the fact that protein
86 cross-linked to an over-digested 1-3 base fragment of RNA (~0.3-1 kDa) will run so close to
87 un-cross-linked protein that it would not be distinct for a ~70 kDa protein[2].
88
89 One of the common questions in molecular biology is whether there are specific RNA
90 interactions for a protein of interest, and what those RNAs are. However, there is no
91 agreement on what constitutes a target RNA, and interactions occur along a continuum of
92 affinities[3]. One potential criterion for a specific RNA interaction for a protein of interest is those
93 interactions with a frequency per protein or fraction of interactions unlikely to occur with a
94 randomly selected protein. Neither of these definitions have been used because no library of
95 random non-RBP RNA-interactomes have been analyzed. One of the goals of this study was
96 to enable target RNAs to be defined in these two ways.
97
98 Here we report an improvement to current CLIP protocols in an approach termed
99 easyCLIP. easyCLIP reliably quantifies the numbers of RNA cross-links-per-protein and
100 provides visual confirmation of each step in the CLIP protocol. easyCLIP was used to
101 produce data for eleven randomly selected non-RBPs as well as a set of canonical RBPs,
102 allowing us to approximate the distribution of RNA-binding interactions with the average
103 protein and to propose a threshold for assignment of a protein as an RBP.
104
105 Finally, easyCLIP was applied to quantify the mutational impacts on RNA binding of L100
106 PCBP1. L100 PCBP1 missense mutants were highlighted in a recent global analysis of
107 mutations in gastrointestinal adenocarcinoma (GIAC)[4], which characterized a subset of GIAC
108 that were broadly "genome stable" (i.e., lacking chromosome or microsatellite instability), but

possessing frequent mutations in APC, KRAS, SOX9, and PCBP1. Unexpectedly, easyCLIP found the common cancer-associated L100 mutations in *PCBP1* increased the association of PCBP1 with RNA and suggested potential mechanisms for their selective advantage. easyCLIP is thus presented as a new CLIP method with built in verification checks that enables quantification of the number of RNA cross-links per protein to allow quantitative comparison across CLIP datasets.

117 ***Results***

118 **Library preparation by easyCLIP.** To generate a simpler and faster way of producing CLIP-
119 seq datasets, a method was developed using on-bead ligations[5–7] of 3′ adapters (termed
120 L3) and 5′ adapters (termed L5), each with a different fluorescent dye[8] (Figure 1A, B). After
121 running an SDS-PAGE gel and transferring to a nitrocellulose membrane, single- and dual-
122 ligated RNA were clearly visible (Figure 1C). RNA was extracted from the nitrocellulose
123 membrane using proteinase K, purified using oligonucleotide(dT) beads to capture the
124 poly(A) sequence on the L3 adapter, eluted, reverse transcribed, and input directly into PCR
125 (Figure 1A). Major differences from HITS-CLIP include the usage of a chimeric DNA-RNA
126 hybrid for highly efficient ligation (see below), the purification of complexes from a gel by
127 oligo(dT), L5 and L3 barcodes, UMIs, and the direct visualization of ligation efficiencies and
128 finished libraries by infrared dyes (see below).
129
130 This method ("easyCLIP") incorporated several advantages. First, since all that happens after
131 the gel extraction is a quick oligonucleotide(dT) purification and reverse transcription before
132 PCR, there are minimal opportunities for error after the diagnostic step of gel imaging.
133 Second, L5 and L3 barcodes may be used to mark samples and replicates, respectively, and
134 all samples may be combined before running SDS-PAGE. This combination of samples
135 allows for lower complexity preparations to "piggy-back" on higher complexity preparations,
136 which allows very small RNA quantities that may be lost to sample absorption to be converted
137 into libraries and for diagnostics from the larger libraries to be used for the smaller.
138
139 easyCLIP was benchmarked against eCLIP in the manner eCLIP was benchmarked against
140 iCLIP, namely using Rbfox2, 10 µg antibody, and 20 million 293T cells. easyCLIP was more
141 efficient than the published eCLIP results (Figure S1A), and easyCLIP RBFOX2 libraries fit
142 expectations, including matching the pattern of binding seen with eCLIP at NDEL1 (Figure
143 S1B), indicating that easyCLIP captures similar information. easyCLIP was then used to
144 generate data for seven additional known RBPs: FBL (Fibrillarin, which associates with C/D-
145 box snoRNA and other ncRNA), hnRNP C, hnRNP D, Rbfox1, CELF1, SF3B1 and PCBP1
146 (all of which at least partly bind mRNA). These were chosen as representatives (FBL, hnRNP
147 C), for their importance to cancer (SF3B1, PCBP1), for comparison with eCLIP (Rbfox2), or
148 by using a random number generator to select RBPs at random from the RBP atlas[9] (Rbfox1,
149 CELF1, hnRNP D). No randomly selected or representative RBPs were discarded.
150
151 easyCLIP libraries produced high quality data in each case (Figure 1D-J, Files 2-5). First, the
152 data was consistent between replicates but distinct between proteins (Figure 1D). Second,
153 FBL and hnRNP C/hnRNP D were un-correlated (Figure 1D), as expected. The data was
154 high quality enough for all eight RBPs that simply feeding the sequences under the tallest
155 1,000 peaks (10,000 for CELF1) to a *de novo* motif discovery program[10] resulted in the top
156 motif being the expected motifs for all eight proteins, despite not performing any statistical
157 tests, normalization, or comparison to a control (Figure 1E). This indicates easyCLIP data is
158 clean enough that no statistical methods or controls are necessary to obtain good quality
159 peaks. Using enrichment over controls also recovered all eight motifs (Figure 1F).
160
161 The motif obtained for FBL is expected because it is similar to the boxes of C/D box
162 snoRNAs. As expected, hnRNP C, hnRNP D, CELF1, Rbfox1, and Rbfox2 bound mostly

mRNA, while FBL was mostly crosslinked to snoRNA and snRNA (Figure 1G). PCBP1 and SF3B1 bound to both mRNA and snRNA, as expected. The main surprise was the appearance of tRNA-binding by PCBP1, addressed further below. About ~90% of hnRNP C/hnRNP D mRNA reads were intronic, as expected (Figure 1H). Under a highly stringent FDR<10^{-4} *vs* random non-RBPs (discussed below), target RNA numbers (Figure 1I) and the total number of unique mapped reads were both similar to what is typical for CLIP studies (Figure S1C); inputs ranged from a fraction of a 10 cm plate (Rbfox2, hnRNP C), to one 15 cm plate (PCBP1).

It is sometimes argued that iCLIP methods and their derivatives have higher resolution because the stop point of reverse transcriptase is mapped, but it has been shown that deletions in CLIP-seq reads also map binding sites to the same resolution[11]. For a very short RNA, such as a snoRNA, binding sites over much of the RNA are too close the 3' end to be mappable, making the binding site ambiguous. However, using deletions allows binding sites anywhere in the RNA to be identified. Cross-linking positions within C/D box snoRNA were visualized in some detail (Figure 1J), and the respective frequencies of crosslinking in the different regions of C/D box snoRNAs matched previous reports[12]. This indicates easyCLIP provides an advantage over iCLIP/eCLIP-like methods for short RNAs, where reads with reverse transcriptase stops near the 3' end are not mappable.

Estimating absolute RNA quantities. easyCLIP was next tested to see if it could determine the total amount of RNA crosslinked to a given protein. Prior work has ligated 3′ adapter molecules labelled with infrared dyes to count crosslinked RNAs[8], but this method does not account for un-ligated RNA, and is only accurate if there are no changes in dye fluorescence during the procedure or from imaging conditions.

When HEK293T cells were UV-crosslinked, hnRNP C immunopurified and RNA highly digested, a series of bands were visible by western blot (Figure 2A), spaced at roughly the ~60 kDa size of an hnRNP C dimer, as not all cross-linked complexes can be collapsed to monomers by RNAse digestion. If a ~15 kDa fluorescent adapter was ligated to highly digested hnRNP C-crosslinked RNA, a new band ~15 kDa above monomeric hnRNP C appeared containing adapter and hnRNP C (Figure 2B). The amount of protein in this band was determined by quantitative western blotting (Figure 2C, Figure S2A). The concentrations of standards were determined using multiple methods (Figure S2B-E), and consistency was established between epitope standards (Figure S2F). To determine if the hnRNP C antibody used (4F4) discriminated between non-cross-linked and cross-linked hnRNP C, epitope tagged hnRNP C was *in vitro* crosslinked to RNA, and 4F4 antibody showed only a negligible 16% bias (Figure S2G). Because the cross-linked band (Figure 2B) contains an equal number of protein and RNA molecules, quantification of the amount of protein in the cross-linked band relates adapter fluorescence values in this band into an absolute molecule number. Quantification of fluorescence per molecule using a single, large preparation of cross-linked, quantified hnRNP C as an aliquoted standard can be used to translate fluorescence values to RNA quantities if the loss is fluorescence is low and the ligation efficiency can be approximated.

208 **Fluorescence loss.** To address the loss in adapter fluorescence from CLIP, a method was
209 developed to determine this value for labelled DNA oligonucleotides. Antisense
210 oligonucleotides to L5 and L3 were labelled with reciprocal dyes, hereafter termed αL5 and
211 αL3, and used to shift their cognate adapter. That is, a red αL3 and a green αL5 are used to
212 shift a green L3 and red L5. Such antisense oligonucleotides shift the adapter molecules up
213 in a native gel and produce bands of both colors with a 1:1 ratio of antisense and sense
214 oligonucleotide (Figure 2D). L5 and L3 were successfully purified from proteinase K extract
215 and RNAse digested down to free adapters (Figure 2E). 100% of L5 and L3 adapters were
216 shifted in this manner (Figure 2F) and the method was applied to the RNAse digested CLIP
217 oligonucleotides (Figure 2G). By comparing the ratio of αL5 to L5 for fresh L5 and L5
218 extracted from the nitrocellulose membrane in CLIP, the loss in L5 fluorescence from CLIP
219 could be determined (Figure 2H). L5 consistently lost only ~20% of its fluorescence.
220
221 **Ligation efficiency.** Three methods were used to estimate ligation efficiency. The most
222 straightforward of these is to ligate both a fluorescent L5 and L3 adapter and visualize the
223 single *vs* dual shift from one or both adapters being ligated (Figure 3A). By quantifying the
224 amount of fluorescence signal in the single- and dual-ligated protein-RNA complexes,
225 efficiency estimates are obtained for both 5′ and 3′ (Figure 3B and C). Assuming the two
226 ligations are independent events, the total amount of crosslinked RNA is also obtained,
227 including unlabeled RNA (Figure 3C). This method indicated that L5 ligation efficiencies were
228 consistent and in the neighborhood of 50% (Figure 3D).
229
230 It was hypothesized that the higher molecular weight complexes visible in Figure 3A were
231 produced by variation in the crosslinked protein, such as multimeric hnRNP C. If so, then the
232 removal of protein by proteinase K digestion would remove the additional bands. To test this,
233 RNA was extracted from nitrocellulose membranes using proteinase K, purified using either
234 L5 or L3, run on a polyacrylamide gel, and transferred to a nylon membrane. Consistent with
235 this hypothesis, higher molecular weight bands were collapsed into two simple smears of
236 fluorescence, corresponding to mono-ligated and dual-ligated RNA (Figure 3E). A similar
237 logic as applied in Figure 3A-C was applied to the protein-free RNA in Figure 3E to produce
238 estimates of ligation efficiencies, which were lower but also consistent between replicates
239 (Figure 3D, F).
240
241 A third method was also employed to quantify ligation efficiencies. Because the shifted bands
242 in Figure 2G have a 1:1 ratio of L:αL oligonucleotides, quantifying antisense oligonucleotides
243 also quantifies their respective adapters. The development of an antisense oligonucleotide-
244 based method to quantify low femtomole amounts of adapter necessitated some
245 optimization, described in Figures S3-8 and associated legends. For example, diluent has
246 dramatic effects on fluorescence (Figure S5A) and there was a systematic test of the effects
247 of salt, carrier, and PEG to retain fluorescence, prevent sample loss from adhesion, and
248 preserve complexes on a gel (Figure S5B-F). Shifting known concentrations of L5 and L3
249 adapter fit well to a linear model, typically within 3 fmols (Figure S8C-D). By this third method,
250 L5 ligation efficiencies were ~70% and consistent between CLIP rounds (Figure 3D). From
251 these three methods, L5 ligation rates are stable between experiments and are roughly
252 50±20%. Altogether, results on the loss of adapter fluorescence (Figure 2) and ligation

253 frequency (Figure 3) supported the use of standard aliquots (Figure 2B) to quantify absolute
254 RNA amounts in CLIP experiments.
255
256 **Crosslink rates for RBPs.** Two measures of RNA cross-linked to protein were determined:
257 all RNA and minimal region RNA (Figure 4A). "All RNA" reflects the cross-linked RNA on the
258 nitrocellulose membrane at the minimum size for a small protein-L5 complex (~30 kDa) and
259 everything larger. Co-purified proteins cross-linked to RNA contribute to the total cross-linked
260 RNA visualized. However, these are useful numbers because (1) since co-purified proteins
261 must survive stringent purification conditions, they must constitute a close interaction of the
262 protein of interest with RNA, and (2) the protein of interest often runs at a range of sizes (i.e.
263 hnRNP C). The "minimal region" RNA measurement is taken from the region corresponding
264 to the size for the dominant protein band cross-linked to small RNA fragments and ligated to
265 L5, a region more likely to correspond to direct cross-linking events (Figure 4A). For all RNA,
266 hnRNP C and FBL were 37% and 7% crosslinked to RNA, respectively (Figure 4B, see
267 Figure S2H-I for FBL quantitative western blotting). Cross-link rates for the RBPs hnRNP D
268 (19%), Rbfox1 (40%), CELF1 (21%), STAU1 (4.9%), PCBP1 (0.5%) and eIF4H (0.3%) were
269 also established (Figure 4B). Cross-links in the minimal region (Figure 4C) were determined
270 for RBPs hnRNP C (22%), FBL (2%), Rbfox1 (18%), CELF1 (11%) hnRNP D (5%), STAU1
271 (1.2%), PCBP1 (0.2%) and eIF4H (0.2%). STAU1 has a reputation as a very poor cross-
272 linker[13], so its cross-link rate may be taken as a representative for such.
273
274 The accuracy of this method was tested by calculating the cross-link rate of hnRNP C by
275 quantitative western blotting of immunopurified hnRNP C (Figure S9). Results from this
276 method agreed to within ~10%. It was asked if easyCLIP would reflect a loss in RNA-binding
277 affinity caused by the F54A mutant of hnRNP C, a mutation in the RNA-binding surface of
278 the RRM that elevates the RRM's *in vitro* K_D from ~1 μM to >20 μM[14]. The mutant was
279 dramatically less cross-linked (Figure 4C, $P<0.05$ t-test), although it still cross-linked better
280 than the average human non-RBP (discussed below), consistent with hnRNP C functioning
281 in a complex and possessing RNA contacts outside the RRM.
282
283 **Cross-link rates for non-RBPs.** Quantification of cross-link rates may identify a numerical
284 threshold for distinguishing RBPs from non-RBPs and for determining when an RBP has lost
285 or gained RNA-binding activity. To derive a distribution of cross-link rates for non-RBPs, 11
286 non-RBP proteins were randomly selected using a script. This set of randomly selected non-
287 RBPs cover a diverse range of functions and subcellular locations (Figure 4C-D). Selected
288 non-RBPs had total RNA crosslink values of 0.03-2% (Figure 4F-G, Figure S10), and rates
289 correlated with protein size (Figure S10B). Reducing counts to minimal region RNA dropped
290 all cross-link rates except UBA2 to below 0.1%, and UBA2 to 0.16% (Figure 4G).
291
292 **Cross-linking rates distinguish RBPs and non-RBPs.** Data above indicate that cross-link
293 rates derived from a minimal region are typically below 0.1% for non-RBPs and above 0.1%
294 for RBPs. The amount of total cross-linked RNA purified, not just that in the minimal region,
295 ranges greatly (non-RBPs 0.1-2%, RBPs 0.2-42%). These metrics can be used to aid in
296 defining what proteins are RBPs. For example, FHH-hnRNP C F54A had a minimal region

297 cross-link rate of 0.1%, consistent with losing most direct affinity for RNA but still joining an
298 RNA-binding complex.
299
300 **Defining specific interactions of RBPs and non-RBPs.** One of the goals of this study was
301 to enable target RNAs to be defined for a protein of interest as those interactions with a
302 frequency per protein or per-cross-link unlikely to occur with a randomly selected protein. To
303 do so, easyCLIP libraries for the ten of the eleven random non-RBPs were prepared. The
304 specificity of the resulting libraries was confirmed by the over-representation of each
305 overexpressed protein's own RNA in CLIP data (Figure S10C). Despite not being RBPs,
306 different non-RBPs produced distinct RNA-interactions (Figure 4H, Figure S10D). The two
307 solely-nuclear proteins UBA2 and ETS2 had a low fraction of mRNA reads (Figure 4H).
308
309 Using the resulting distribution of RNA interactions for random proteins, it is possible to
310 directly estimate how "unusual" any RNA-protein interaction pair is. This method was first
311 applied to interaction frequencies per cross-link (i.e. per read). The validity of this method is
312 supported by the identification of the expected motif for all eight RBPs as the top motif (Figure
313 1F), and target RNA types were consistent with expectations (Figure 1I): FBL targeted
314 snoRNA, while hnRNPs targeted mRNA, and the core snRNP component SF3B1 targeted
315 mRNA and snRNA. The number of FBL mRNA targets at least partly reflects mRNAs
316 containing intronic snoRNAs. For each non-RBP, its own targets were defined after removing
317 it from the set of controls, yet this still resulted in few "target" RNAs.
318
319 Finally, we identified target RNAs as those bound *per protein* at an unusually high rate.
320 Frequent mRNA and lncRNA interactions per protein are characteristic of RBPs (Figure 4H).
321 The rate of cross-linking per protein was plotted as a histogram to all mRNAs (Figure 5, *left*),
322 snoRNAs (*middle*), or tRNA (*right*), which suggested some fundamental results. First, the
323 distribution of binding across mRNAs, in reads-per-million, is similar between RBPs and non-
324 RBPs (*top left*), but RBPs have many more frequent mRNA partners per protein. snoRNA
325 presents a different picture (*middle*). Naïvely, if one looked only at reads-per-million, it would
326 seem that either randomly selected proteins target snoRNA, or else RBPs somehow
327 specifically avoid it. Per-protein, however, mRNA-binding RBPs and non-RBPs are equally
328 likely to contact snoRNA – consistent with only FBL having specific interactions with snoRNA
329 (*bottom middle*). The reason for this is clear enough – mRNA-binding RBPs have additional
330 interactions that decrease the fraction of total interactions that occur with snoRNA. Despite
331 its extremely high cross-link rate to mRNA, hnRNP C cross-links to snoRNA the same a
332 random protein, as expected from such interactions being random. This cautionary tale helps
333 explain the tRNA-binding observed by PCBP1 (Figure 1G). Like snoRNAs, tRNAs make up
334 a disproportionate share of the libraries of non-RBPs (*top right*), but per-protein all RBPs and
335 non-RBPs have the same distribution (*bottom right*). The distribution of tRNA binding by
336 PCBP1 is actually just that of a non-RBP, indicating that it has no evolved interaction with
337 tRNA, as might have been thought from conventional analysis in the absence of randomly
338 selected non-RBPs.
339
340 **Cancer-associated mutations.** The most frequent missense mutations in RBPs were
341 identified in cancer using TCGA data[15] (Figure 6A). The K700E mutant of SF3B1, the
342 L100P/L100Q mutants of PCBP1 (Figure 6B), and the P131L mutant of RQCD1 were

343 selected. SF3B1 K700E and RQCD1 P131L did not have obvious effects on RNA-binding in
344 preliminary experiments, so PCBP1 was focused on for analysis.
345
346 PCBP1 is both transcription factor and RBP, both nuclear and cytoplasmic, and highly
347 multifunctional beyond RNA-binding[16,17]. As a result, PCBP1 was expected to cross-link less
348 than the average RBP. The cross-link rate of wild-type PCBP1 was indeed higher than non-
349 RBPs, but lower than other RBPs (Figure 6C and D). To test if cross-linking was specific,
350 GxxG loop mutations were introduced in all three KH domains of PCBP1, which remove the
351 affinity of KH domains for RNA while allowing the domains to fold properly[18]. "GxxG PCBP1"
352 no longer cross-linked to RNA (<0.01%, Figure 6C).
353
354 The effects of the PCBP1 L100 mutation were next examined. The first and second KH
355 domains of the closely related protein PCBP2 form a pseudo-dimer, in which the β1 and α3
356 elements of both KH1 and KH2 bury hydrophobic residues against the other domain to form
357 an intramolecular dimer[19]. L100, in β1 of KH2, is part of this dimerization surface[19],
358 suggesting L100 mutants might alter conformation to impair RNA-binding.
359
360 Surprisingly, the opposite effect was observed: L100P/Q PCBP1 was three-fold *more* cross-
361 linked to RNA (Figure 6C-E). L100P/Q PCBP1 was dramatically destabilized (Figure 6F,
362 Figure S11). Expressing PCBP1 from a vector containing an upstream ORF that lowered
363 expression to below that of L100P/Q PCBP1 (Figure 6F) did not substantially increase cross-
364 link rate (Figure 6C, D), ruling out expression levels as the cause of differential RNA-binding.
365 These results indicate most of the wild-type protein is not bound to RNA in HCT116.
366 Interestingly, if the entire KH domain containing L100 (KH2) is removed, cross-linking was
367 approximately the same as wild-type (Figure 6C, D), yet ΔKH2 PCBP1 was also destabilized
368 (Figure 6F, Figure S11).
369
370 L100P/Q mutants had a much smaller fraction of reads mapping to snRNA (Figure 6G), and
371 on a per protein basis, L100P/Q greatly increased its association with mRNA (Figure 6H). It
372 was therefore hypothesized that L100P/Q PCBP1 was more cytoplasmic than wild-type
373 PCBP1, which was confirmed by microscopy (Figure S12, Figure 6I). ΔKH2's location was
374 unaltered (Figure S12).
375
376 The quantifications done by easyCLIP allow for new insight, as three different views of RNA-
377 protein interactions are enabled (Figure 6J-N). Binding to snRNA by L100 PCBP1 is reduced
378 per protein, but on a per cell basis it is clear the snRNA association of PCBP1 collapses in
379 the L100P/Q mutants (Figure 6J, M). Although mutant PCBP1 interacts more often with
380 mRNA per protein, per cell it is similar (Figure 6J, K, L). We note that the increase in GSK3A
381 association is strong enough to overcome the effect of reduced abundance (Figure 6L).
382 Altogether, Figure 5 and Figure 6J-N highlight the complexity of RNA-protein interactions,
383 and how misled one might be if restricted only to analyzing CLIP data on the traditional basis
384 of read distributions.
385
386 ***Discussion***
387 easyCLIP provides a general method for estimating RNA-per-protein cross-link rates.
388 easyCLIP is easy, fast, reliable, and efficient. It provides direct visualization of the success of

389 library preparation steps, allows multiplexing based on two adapters, and determines ligation
390 efficiency. A major limitation to this approach is its reliance on UV cross-linking as a proxy for
391 *in vivo* interactions[20].
392
393 These PCBP1 results are consistent with a model where the L100P/Q mutations impair the
394 stabilizing effect of KH2 and have a gain-of-function for KH2 with regards to location and
395 RNA-binding. To the author's knowledge, this is the first time a disease-associated mutation
396 in an RBP has resulted in increased RNA-association.
397
398 PCBP1 protein is often down-regulated in cancer, which aids in tumorigenesis[21]. It is likely
399 that the L100P/Q mutations contribute to tumorigenesis at least partly by destabilizing
400 PCBP1. However, L100P/Q is only observed at high frequency in colon and rectal
401 adenocarcinoma and down-regulation cannot explain the selection of a specific missense
402 mutation. PCBP1 has been proposed to suppress tumors by binding mRNA and stabilizing
403 tumor suppressor mRNAs, repressing translation of oncogenic mRNAs, and inhibiting
404 oncogenic splicing[21]. The changes per cell we observe, however, indicate that while the
405 landscape of PCBP1-RNA interactions is radically altered, the number of mRNA-PCBP1
406 complexes are similar with L100 mutants, and rather point to either changes in regulatory
407 effect or a loss of function in splicing.
408
409 ***Methods***
410 The easyCLIP protocol is described in File S1 with additional information in Supplementary
411 Methods. Full methods are in the Supplementary Methods section. High-throughput
412 sequencing data is under the GEO accession GSE131210.
413
414 ***Acknowledgments***
415 We thank Brian Zarnegar for reagents, and input on experiments and their interpretation. We
416 thank Amin Zia for performing analysis of TCGA data to identify missense mutations in RBPs
417 in cancer. We thank Zurab Siprashvili and Yuning Wei for assistance. The SF3B1 sequence
418 was obtained from a vector produced by Angelos Constantinou, provided by Marc-Henri
419 Stern. Funding was provided by the NIAMS/NIH grant 1F32AR072504 to D.F.P., NIAMS/NIH
420 grants AR45192, AR007422 and AR49737 to P.A.K., and by a USVA Merit Review grant to
421 P.A.K. Some data was generated on an Illumina HiSeq 4000 purchased with funds from NIH
422 award S10OD018220 by SFGF at Stanford.
423
424 ***Author Contributions***
425 D.F.P. wrote the software and conceived, designed, performed and analyzed all
426 experiments. P.K. and D.F.P. planned experiments and wrote the paper.
427
428 ***Declaration of Interests***
429 The authors declare they have no competing interests.
430
431

References

1. Chakrabarti, A. M., Haberman, N., Praznik, A., Luscombe, N. M. & Ule, J. Data Science Issues in Studying Protein–RNA Interactions with CLIP Technologies. *Annu. Rev. Biomed. Data Sci.* **1**, 235–261 (2018).
2. Janes, K. A. An analysis of critical factors for quantitative immunoblotting. *Sci. Signal.* **8**, rs2 LP-rs2 (2015).
3. Jarmoskaite, I. *et al.* A Quantitative and Predictive Model for RNA Binding by Human Pumilio Proteins. *Mol. Cell* (2019). doi:https://doi.org/10.1016/j.molcel.2019.04.012
4. Liu, Y. *et al.* Comparative Molecular Analysis of Gastrointestinal Adenocarcinomas. *Cancer Cell* **33**, 721-735.e8 (2018).
5. Granneman, S., Kudla, G., Petfalski, E. & Tollervey, D. Identification of protein binding sites on U3 snoRNA and pre-rRNA by UV cross-linking and high-throughput analysis of cDNAs. *Proc. Natl. Acad. Sci.* **106**, 9613 (2009).
6. Porter, D. F., Koh, Y. Y., VanVeller, B., Raines, R. T. & Wickens, M. Target selection by natural and redesigned PUF proteins. *Proc. Natl. Acad. Sci. U. S. A.* **112**, 15868–15873 (2015).
7. Benhalevy, D., McFarland, H. L., Sarshad, A. A. & Hafner, M. PAR-CLIP and streamlined small RNA cDNA library preparation protocol for the identification of RNA binding protein target sites. *Protein-RNA Struct. Funct. Recognit.* **118–119**, 41–49 (2017).
8. Zarnegar, B. J. *et al.* irCLIP platform for efficient characterization of protein—RNA interactions. *Nat. Methods* **13**, 489–492 (2016).
9. Castello, A. *et al.* Insights into RNA Biology from an Atlas of Mammalian mRNA-Binding Proteins. *Cell* **149**, 1393–1406 (2012).
10. Heinz, S. *et al.* Simple combinations of lineage-determining transcription factors prime cis-regulatory elements required for macrophage and B cell identities. *Mol. Cell* **38**, 576–589 (2010).
11. Zhang, C. & Darnell, R. B. Mapping in vivo protein-RNA interactions at single-nucleotide resolution from. *Nat. Biotechnol.* **29**, 607–614 (2011).
12. Kishore, S. *et al.* Insights into snoRNA biogenesis and processing from PAR-CLIP of snoRNA core proteins and small RNA sequencing. *Genome Biol.* **14**, R45–R45 (2013).
13. Kim, B. & Kim, V. N. fCLIP-seq for transcriptomic footprinting of dsRNA-binding proteins: Lessons from DROSHA. *Methods* (2018). doi:https://doi.org/10.1016/j.ymeth.2018.06.004
14. Cieniková, Z., Damberger, F. F., Hall, J., Allain, F. H.-T. & Maris, C. Structural and Mechanistic Insights into Poly(uridine) Tract Recognition by the hnRNP C RNA Recognition Motif. *J. Am. Chem. Soc.* **136**, 14536–14544 (2014).
15. Network, T. C. G. A. R. *et al.* The Cancer Genome Atlas Pan-Cancer analysis project. *Nat. Genet.* **45**, 1113 (2013).
16. Meng, Q. *et al.* Signaling-dependent and coordinated regulation of transcription, splicing, and translation resides in a single coregulator, PCBP1. *Proc. Natl. Acad. Sci. U. S. A.* **104**, 5866–5871 (2007).
17. Makeyev, A. V & Liebhaber, S. A. The poly(C)-binding proteins: a multiplicity of functions and a search for mechanisms. *RNA* **8**, 265–278 (2002).

478 18. Hollingworth, D. *et al.* KH domains with impaired nucleic acid binding as a tool for
479 functional analysis. *Nucleic Acids Res.* **40**, 6873–6886 (2012).
480 19. Du, Z., Fenn, S., Tjhen, R. & James, T. L. Structure of a Construct of a Human
481 Poly(C)-binding Protein Containing the First and Second KH Domains Reveals
482 Insights into Its Regulatory Mechanisms. *J. Biol. Chem.* **283**, 28757–28766
483 (2008).
484 20. Ramanathan, M., Porter, D. F. & Khavari, P. A. Methods to study RNA–protein
485 interactions. *Nat. Methods* **16**, 225–234 (2019).
486 21. Guo, J. & Jia, R. Splicing factor poly(rC)-binding protein 1 is a novel and
487 distinctive tumor suppressor. *J. Cell. Physiol.* **234**, 33–41 (2019).
488

Fig 1

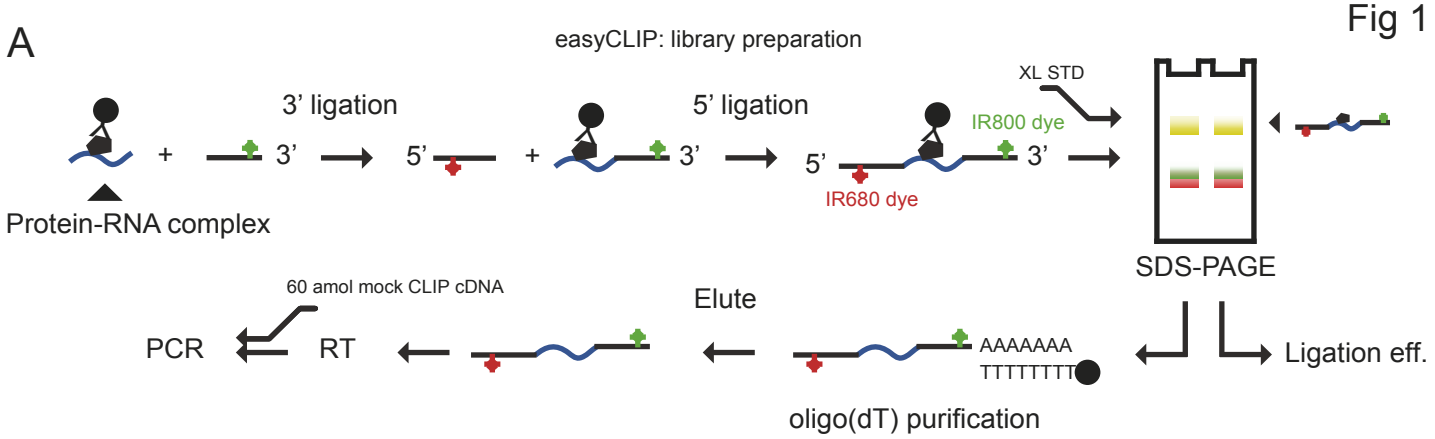
A
easyCLIP: library preparation
3' ligation
5' ligation
XL STD
IR800 dye
IR680 dye
Protein-RNA complex
SDS-PAGE
60 amol mock CLIP cDNA
Elute
PCR
RT
AAAAAAA
TTTTTTTT
Ligation eff.
oligo(dT) purification

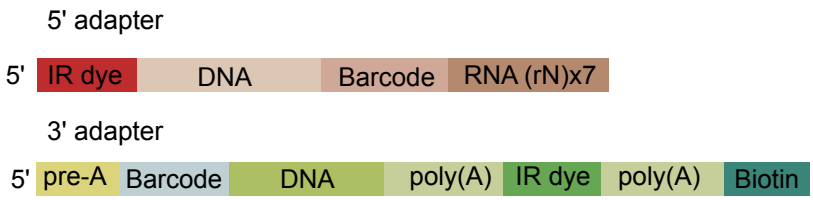
B
5' adapter
5'
IR dye
DNA
Barcode
RNA (rN)x7
3' adapter
5'
pre-A
Barcode
DNA
poly(A)
IR dye
poly(A)
Biotin

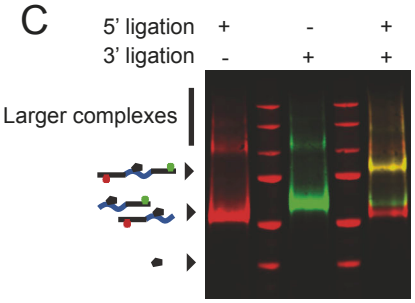
C
5' ligation + - +
3' ligation - + +
Larger complexes

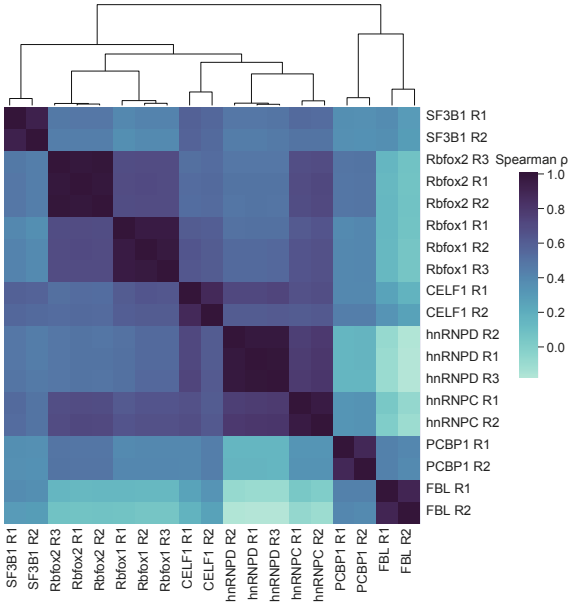
D
Spearman ρ
1.0
0.8
0.6
0.4
0.2
0.0
SF3B1 R1
SF3B1 R2
Rbfox2 R3
Rbfox2 R1
Rbfox2 R2
Rbfox1 R1
Rbfox1 R2
Rbfox1 R3
CELF1 R1
CELF1 R2
hnRNPD R2
hnRNPD R1
hnRNPD R3
hnRNPC R1
hnRNPC R2
PCBP1 R1
PCBP1 R2
FBL R1
FBL R2

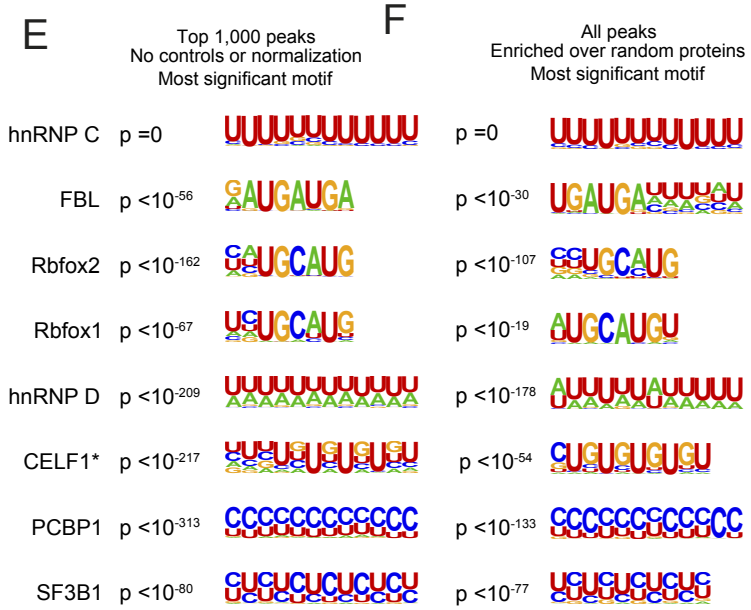
E
Top 1,000 peaks
No controls or normalization
Most significant motif
F
All peaks
Enriched over random proteins
Most significant motif
hnRNP C p =0 p =0
FBL p <10-56 p <10-30
Rbfox2 p <10-162 p <10-107
Rbfox1 p <10-67 p <10-19
hnRNP D p <10-209 p <10-178
CELF1* p <10-217 p <10-54
PCBP1 p <10-313 p <10-133
SF3B1 p <10-80 p <10-77

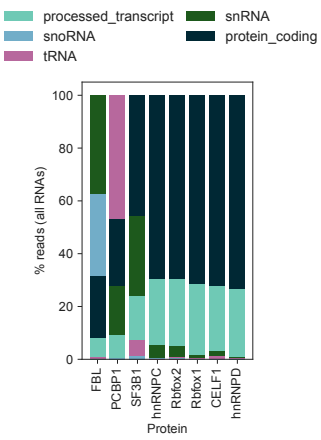
G
processed_transcript
snoRNA
tRNA
snRNA
protein_coding
% reads (all RNAs)
Protein
FBL
PCBP1
SF3B1
hnRNPC
Rbfox2
Rbfox1
CELF1
hnRNPD

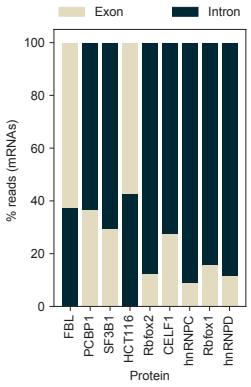
H
Exon
Intron
% reads (mRNAs)
Protein
FBL
PCBP1
SF3B1
HCT116
Rbfox2
CELF1
hnRNPC
Rbfox1
hnRNPD

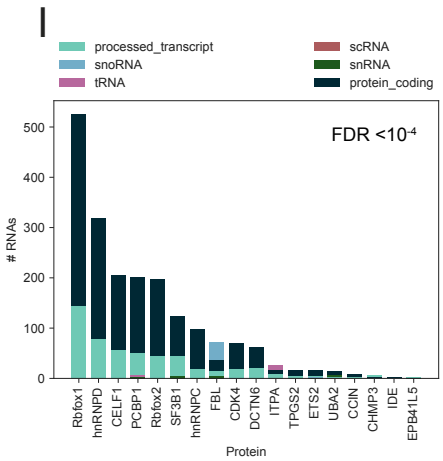
I
processed_transcript
snoRNA
tRNA
scRNA
snRNA
protein_coding
FDR <10-4
RNAs
Protein
Rbfox1
hnRNPD
CELF1
PCBP1
Rbfox2
SF3B1
hnRNPC
FBL
CDK4
DCTN6
ITPA
TPGS2
ETS2
UBA2
CCIN
CHMP3
IDE
EPB41L5

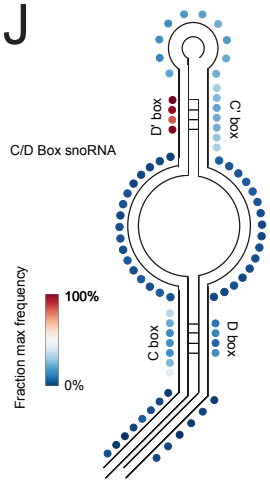
J
C/D Box snoRNA
D' box
C' box
C box
D box
Fraction max frequency
100%
0%

Absolute quantification of ligated RNA

Fig 2

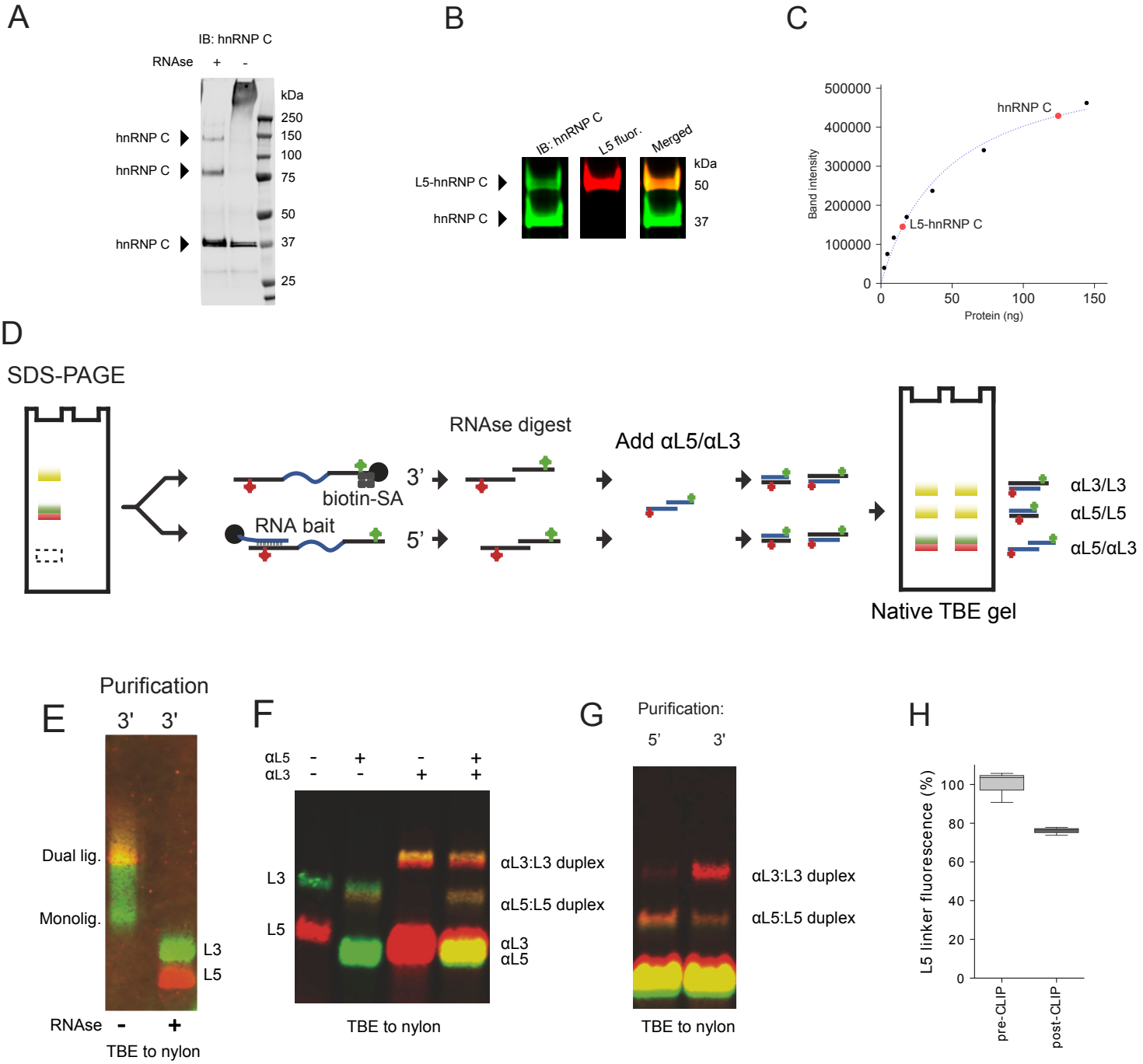

Fig 3

Accounting for ligation efficiency

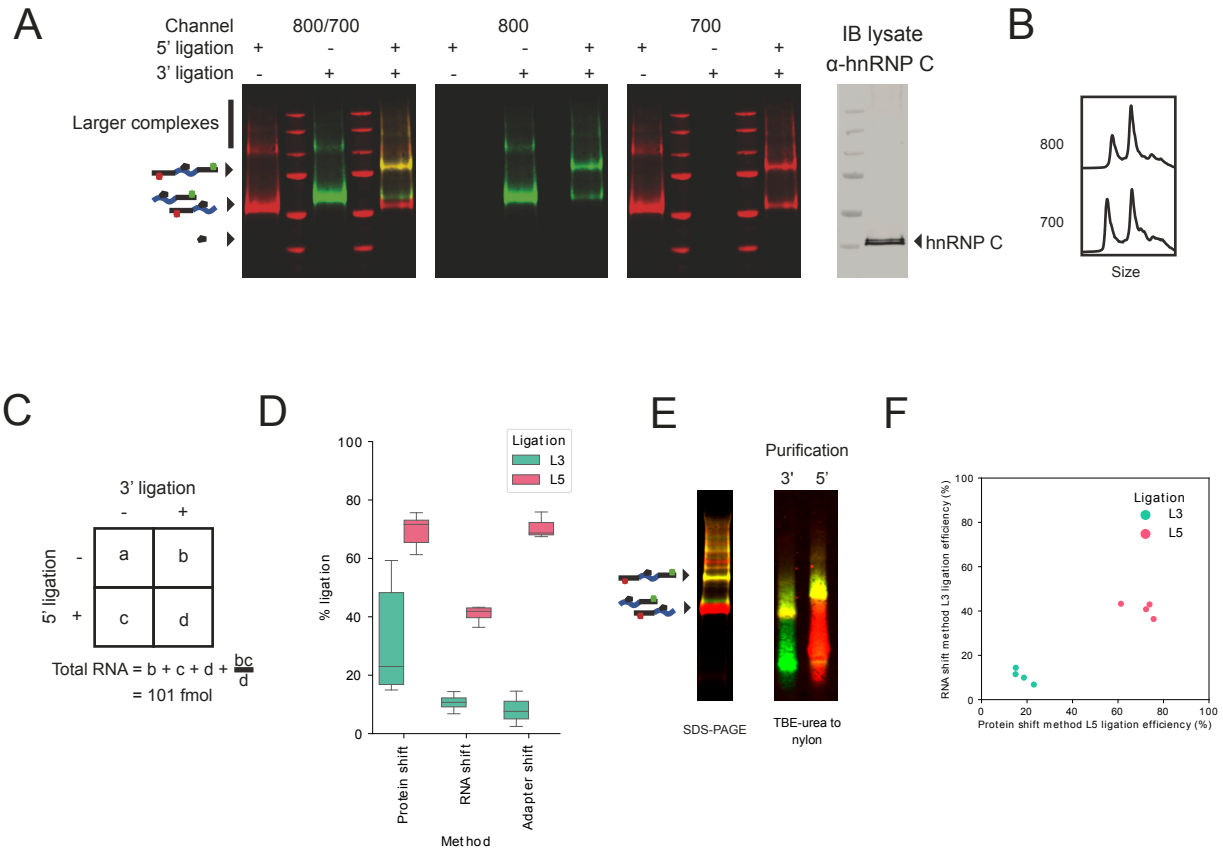

RNA cross-link rates for RBPs and non-RBPs are both diverse and distinct

Fig 4

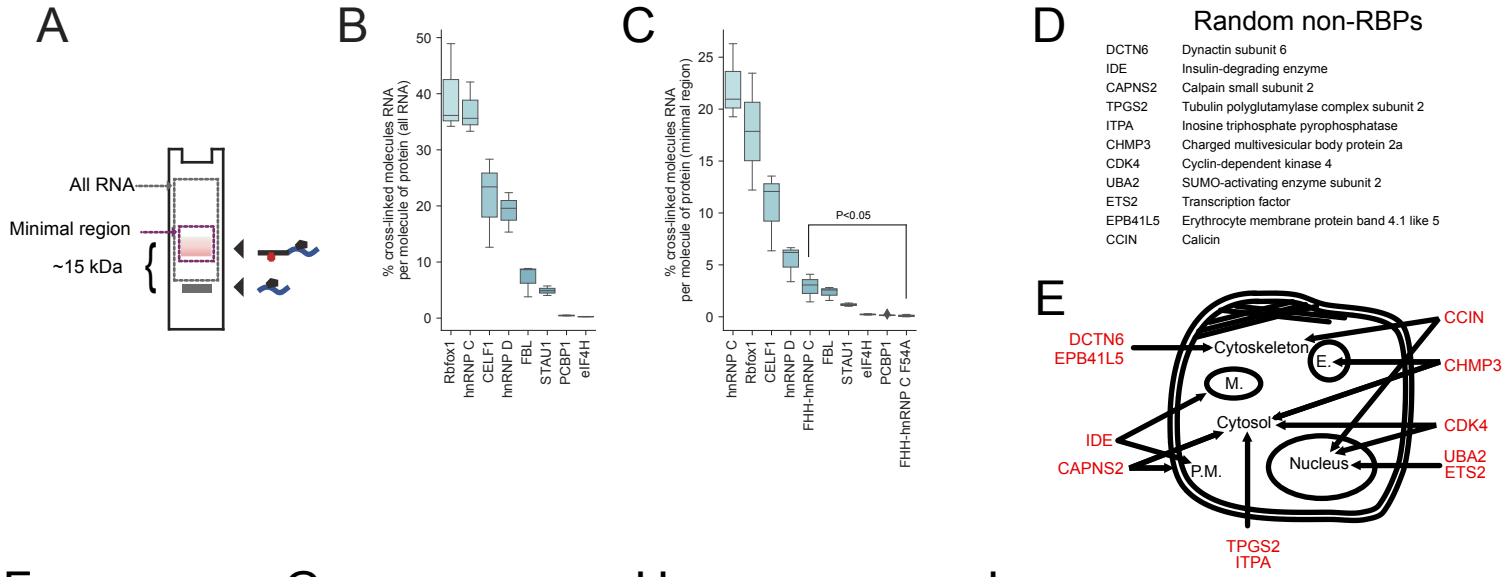

Defining specific interactions for RBPs and non-RBPs by random protein sampling

Fig 5

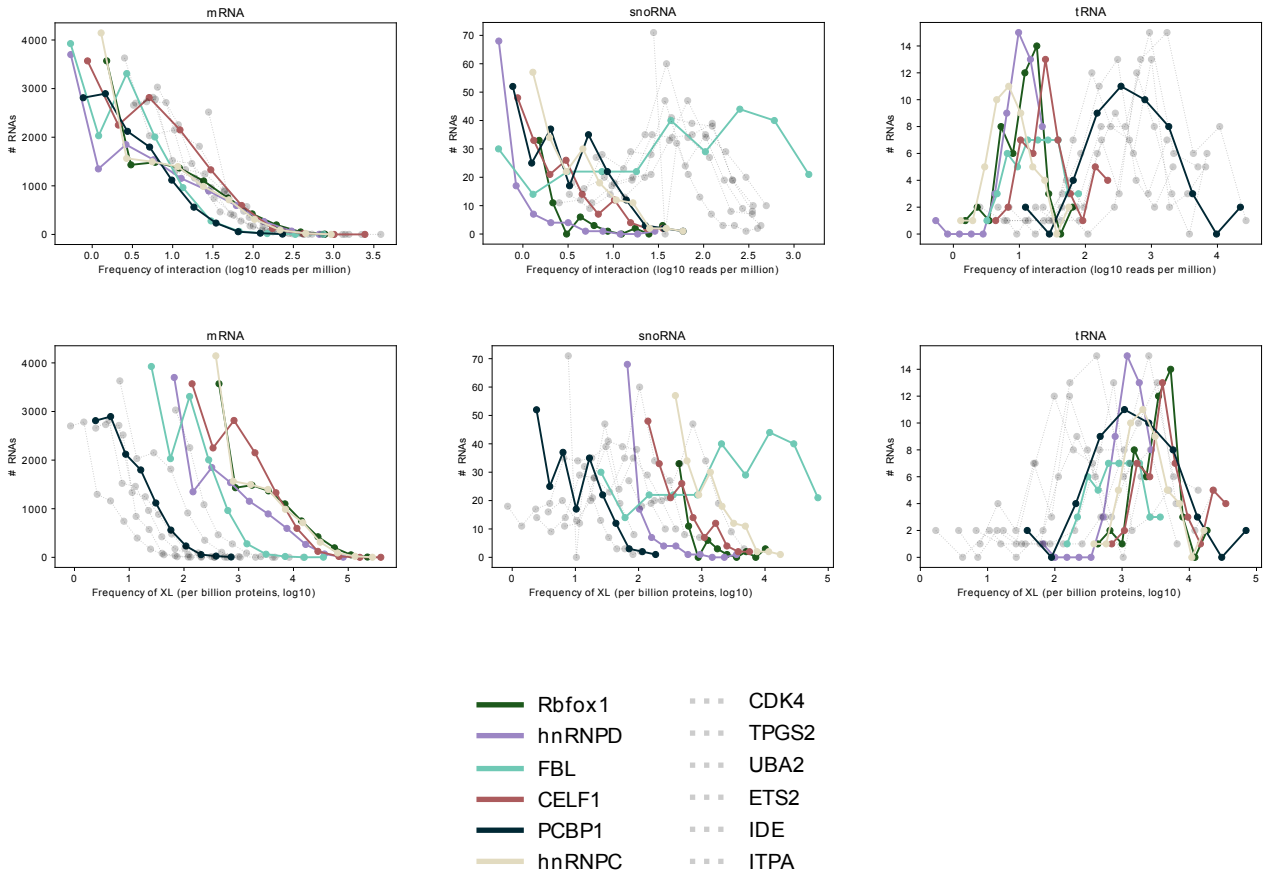

Fig 6

A

The most frequent RBP missense mutations in cancer

Gene	Mutation	# cases/10,161	Mutation rank
SMAD4	R361H	21	81
RARS2	R6C	16	124
SF3B1	K700E	16	137
SMAD4	R361C	14	152
UPF2	E1033D	13	173
PCBP1	L100Q	13	175
SF3B1	R625H	12	200
RQCD1	P131L	12	205
PRKDC	R2522Q	11	231
XPO1	E571K	10	259

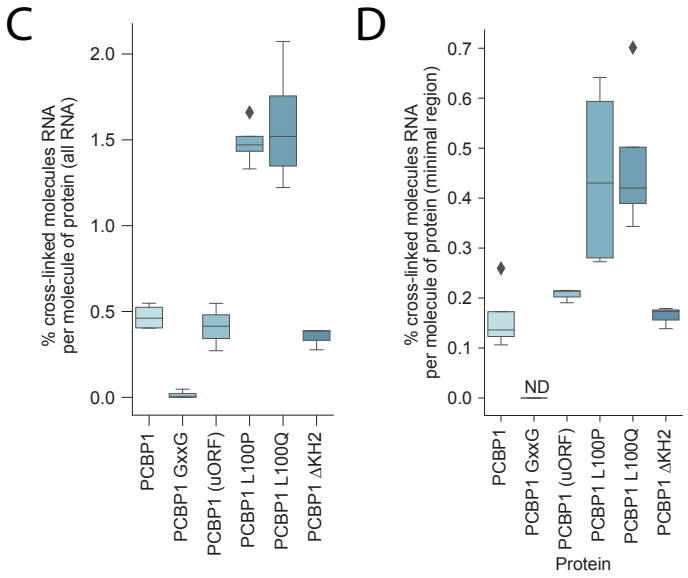

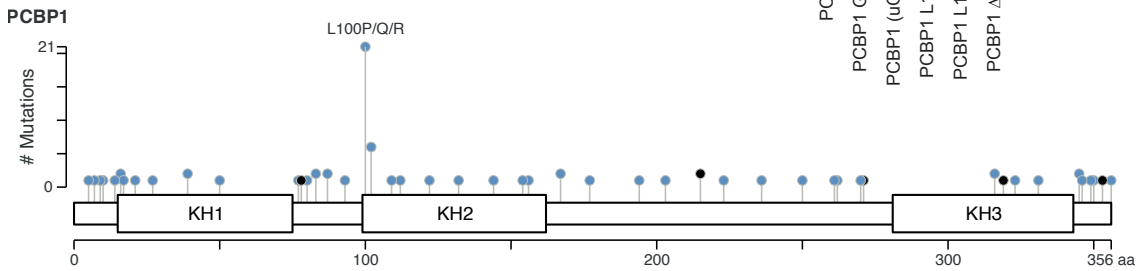

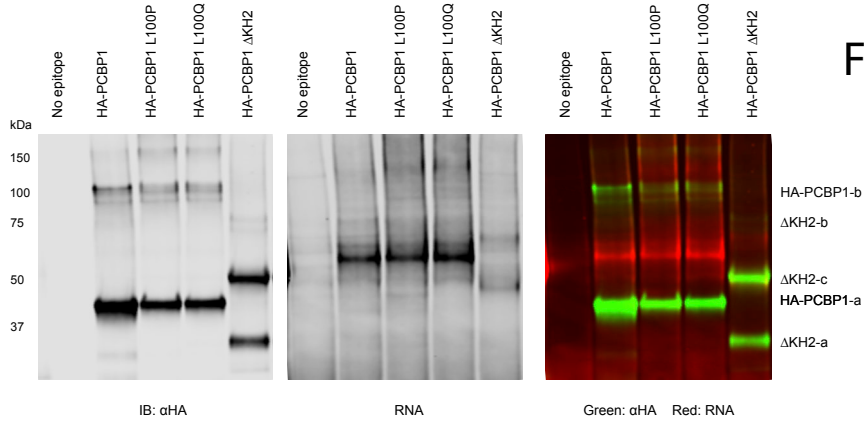

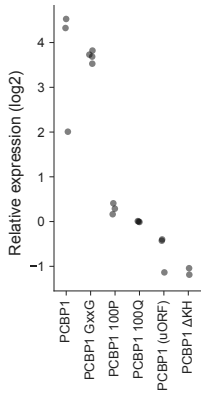

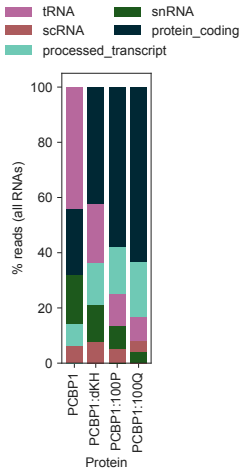

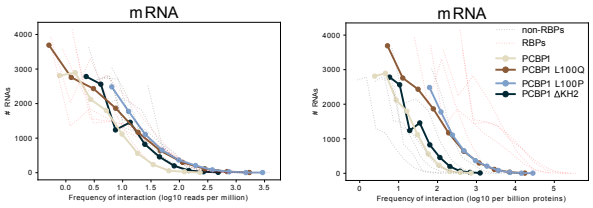

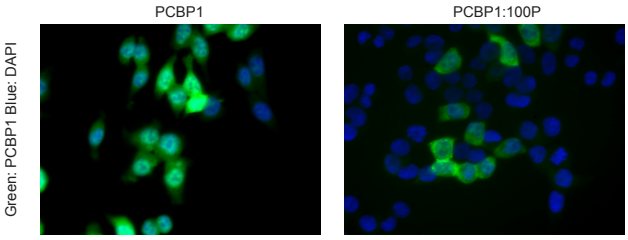

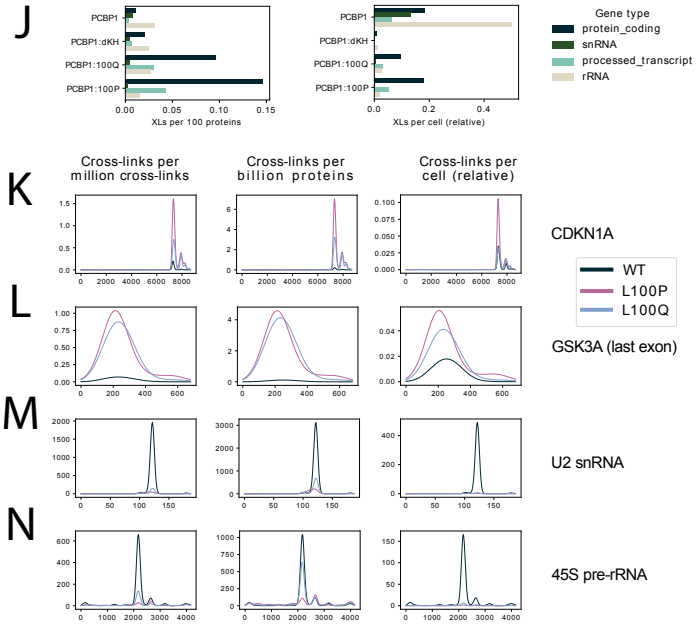

1 **Supplementary material**
2
3 **Supplementary files**
4 **File 1** The full easyCLIP protocol and oligonucleotide sequences.
5
6 **File 2** Description of high-throughput sequencing datasets included in this study.
7
8 **File 3** Raw counts, counts per million reads, and counts per ten billion proteins for all proteins.
9
10 **File 4** P values for all proteins across all RNAs, determined by negative binomial fits to
11 random non-RBPs in all cases.
12
13 **File 5** Peak locations for all proteins in all RNAs.

Supplementary figures

Figure S1 A Comparison of easyCLIP with eCLIP. The comparison used the same amount of the same anti-RBFOX2 antibody, the same cell line, and the same number of cells to perform easyCLIP on RBFOX2. eCLIP produced 72 fmols of library after 16 PCR cycles per replicate, as reported[1], while easyCLIP produced ~13,000 fmols of library after the same number of cycles per replicate (n=3, extrapolating from PCR amplification of 16% of RT reactions). E.L. Van Nostrand *et al.* state that at 100% PCR efficiency their largest replicate would reach 100 fmol after 13 PCR cycles[1]. Dividing 100 fmol by 2^{13} gives an initial library size of 12 amol for eCLIP (7 million molecules) and a PCR efficiency of 86%. The subsequent information on RBFOX2 mapping in E.L. Van Nostrand *et al.*[1] could not have come from this benchmark sample, as the authors report 85% unique reads at 20 million reads sequencing depth, impossible with a starting library of 7 million. eCLIP performed a size selection on their amplified library before sequencing, so the fraction of the input 12 amol that was usable is unknown. This easyCLIP sample did not undergo size selection before sequencing, resulting in many inserts too small to map, but 16% of reads were mappable. If easyCLIP PCR was 96% efficient (*vs* 86% for eCLIP), the starting pool would still be 370 amols. RBFOX2 data was obtained without substantial optimization (three RNAse concentrations were tried) – suggesting RBFOX2 does not represent an optimal case but a typical case. **B** Snapshot of the IGV browser viewing easyCLIP RBFOX2 reads at the same NDEL1 locus as shown in E.L. Van Nostrand *et al.*[1] Figure 1D, showing identification of the same binding sites. Note that the scale bar in E.L. Van Nostrand *et al.* is reads per million, while the scale here is simply raw reads. Reads are placed according to their 5' end location with a single nucleotide width. The GCATG_+.wig tract in red shows the location of GCATG motifs (the Rbfox2 binding site) on the plus strand, with a value of one placed on GCATG, a value of two placed on TGCATG (a preferred form of the motif), and allowing values to sum. **C** Unique mapped reads for eight RBPs. All data was obtained from 293T cells except PCBP1 was obtained from the colon cancer cell line HCT116. Cellular inputs ranged from below 10 million cells (hnRNP C, exact number not recorded), to 10 million (one RBFOX2 replicate), to 20 million (two RBFOX2 replicates), to a maximum of a 15 cm plate. RBFOX2, FBL, and hnRNP C libraries were obtained from antibodies to the endogenous proteins, the others were obtained from FLAG tag purifications from either constructs either integrated at the AAVS1 locus (PCBP1) or transiently over-expressed from a pLEX vector (the others).

Figure S2 Quantification of purified recombinant protein and its application to absolute quantitation of immunopurified protein in CLIP. **A** Quantification of immunopurified endogenous hnRNP C using a GST-hnRNP C standard. The gel is a western blot probed with antibodies to hnRNP C. Endogenous hnRNP C is smaller than GST-hnRNP C but is shown at the same vertical position in this panel as GST-hnRNP C for visualization. In the graph, black dots represent GST-hnRNP C standards, the blue line is a best fit hyperbolic curve, and the red dot is immunopurified endogenous hnRNP C. **B** Quantification of purified GST-hnRNP C expressed in *E. coli*. GST-tagged hnRNP C was purified from *E. coli* using glutathione resin, and then run next to a standard curve of BSA protein on an SDS-PAGE gel. Gel was stained with Coomaisse and fluorescence measured at 700 nm. In the graph, black dots represent BSA standards, the dotted line is a fit hyperbolic curve, and the red dot represents the purified GST-hnRNP C, its position on the y-axis determined from the standard curve. The larger graph is focused on the lower quantities of GST-hnRNP C, while

the larger graph is the same graph zoomed out to include all standards. **C** Quantification of GST-hnRNP C using a tryptophan-reactive dye (Bio-Rad Stain-Free Gel). Gel was subsequently stained with Coomaisse to determine Coomaisse staining of GST-hnRNP C and BSA was not biased. **D** Coomaisse quantification of purified, recombinant GST-FLAG-HA-His-CSRP2 (GST-FHH-CSRP2), the HA standard. CSRP2 was used in this construct because this fusion protein purifies in very high quantities. The hyperbolic curve fit is as in panel B. **E** Quantification of GST-FHH-CSRP2 using a tryptophan reactive-dye to test for a bias in Coomaisse-staining of the HA standard. No bias was observed. **F** Comparison of the quantification standards for HA and hnRNP C. Dilutions of each standard were run on the same gel and western blotted for GST. The standard curve of each protein stock was used to estimate the quantities of the other stock. The proximity of the dots to the 45° line indicate a good agreement. **G** The 4F4 anti-hnRNP C antibody shows little bias between cross-linked and non-cross-linked hnRNP C. Recombinant GST-hnRNP C (made in-house) was incubated with a poly$(U)_{10}$ RNA oligonucleotide (IDT) and UV cross-linked. The resulting mixture, along with GST-hnRNP C (Abnova) standards was run on a denaturing SDS-PAGE gel and transferred to a nitrocellulose membrane for immunoblotting against hnRNP C (4F4) or GST. No significant difference between anti-GST and anti-hnRNP C antibodies in the ratio of cross-linked to non-cross-linked hnRNP C was observed. **H** Coomaisse quantification of purified, recombinant FBL. Purified FBL protein (Prospec, enz-566) was comprised of FBL amino acids 83-321 with an added 23 amino acid tag added, and the FBL antibody (Bethyl, A303-891A) was made against an immunogen between amino acids 271-321 of FBL. As a result, the purified FBL runs faster than endogenous FBL, but both share the entire immunogen used for immunoblotting. **I** Immunoblot quantification of immunopurified FBL using the recombinant FBL visualized in panel H.

Figure S3. A staple oligonucleotide may be used to shift the antisense oligonucleotides in Figure 2D in a single molecule to determine relative fluorescence and control both adapter quantifications to a single complex.

Figure S4 Fluorescence on nylon and nitrocellulose for dot blots of αL3 and αL5 labelled respectively with IR680RD and IR800CW. Signal remains high on nylon, but decays on nitrocellulose

Figure S5 Developing a method to quantify low fmol amounts of adapter. **A** The choice of dilution solution has a large effect on fluorescence. An equimolar mixture of αL3 and αL5 was dilute to 1 nM in the indicated solutions. 2 µL (2 fmols) of diluted oligonucleotide were then dot blotted on nylon and fluorescence measured on a Li-Cor scanner. Carrier DNA was an equimolar solution of 10, 15, and 35 nucleotide poly(A) oligonucleotides. **B** Fluorescence per fmol of αL3 oligonucleotide after diluting to 10 nM in 50 mM Tris pH 7.5 with the indicated salts and blocking agents. Carrier DNA was an equimolar solution of 10, 15, and 35 nucleotide poly(A) oligonucleotides at the indicated ng/µL concentrations. All PEG solutions had 10 ng/µL carrier DNA. Carrier DNA is not sufficient to block signal loss upon dilution. Both monovalent and divalent salts had similar effects. PEG400 and PEG8000 both preserved signal, and higher concentrations generally worked better. **C** The 10 nM solution in panel B was diluted to 1 nM. PEG400 leads to slightly higher fluorescence than PEG8000. Solutions lacking PEG are not depicted due to low signal to noise ratios. **D** Retention of signal

during a 10-fold dilution. Retention is the fluorescence per fmol of the 1 nM solution divided by the fluorescence per fmol of the 10 nM. The choice of salt has no consistent effect. Higher PEG concentrations are better blocking agents. PEG400 and PEG8000 have a similar performance as blocking agents. **E** The choice of 50 mM NaCl or 10 mM $MgCl_2$ has no effect on oligonucleotide loss during dilution (retention) or on signal per fmol. **F** It is safe to run DNA duplexes on 20% polyacrylamide TBE gels (NuPAGE, 12 well, ThermoFisher) at 16.7% PEG400, but higher concentrations lead to fluorescence loss in the duplex, probably due to unfolding of the DNA duplex.

Figure S6 Signal interference between IR800CW and IR680RD dyes. **A** The IR800CW and IR680RD dyes decrease in fluorescence when tethered to the same complex. An excess of αL5 and αL3 were mixed with 50 fmol of an oligonucleotide bearing one copy each of the L5 and L3 sequences, termed the staple oligonucleotide. αL5 was paired with either labelled or unlabeled αL3 to determine the effect of tethering αL3 near αL5, and the reciprocal case was applied to αL3. Complexes were run on a TBE gel in TBEN buffer (0.5X TBE plus 50 mM NaCl) and transferred to a nylon membrane for quantification. **B** Labelled complexes always traveled higher on the gel (right panel). Each dye shifts ~6 nucleotides higher on a TBE gel.

Figure S7 Performance of streptavidin elution methods. **A** L5 and L3 adapters were ligated together *in* vitro, run on a TBE-urea gel, gel extracted, purified using streptavidin beads (MyOne C1, ThermoFisher), and then eluted by the indicated method. This image shows an example of eluates dot blotted on nitrocellulose. Note the peculiar shape of formamide dots. No fluorescence is observed in buffer alone. Water+biotin elution used 100 nM biotin. Formamide elution was 95% formamide with 10 mM EDTA (as suggested by ThermoFisher, who state elution is >95% by this method). DNAse elution used an excess of DNAse I (Ambion) in the buffer supplied by the manufacturer. **B** Fluorescence quantification of the same linker-linker dimers depicted in panel A after each elution method. “TBE-urea gel” indicates fluorescence in the TBE-urea gel before extraction and streptavidin purification. Heating in water with 100 μM biotin was effectively complete, as it yielded similar L5 (700 nm) fluorescence as DNAse elution, which is likely to be complete, and similar fluorescence overall as formamide elution, which is complete according to the manufacturer (ThermoFisher). **C** Water, formamide and TBE-urea gels all affect relative L5/L3 fluorescence (IR680RD/IR800CW). The ratio of dye molecules is 1:1 in all cases, as all cases represent linker-linker dimers.

Figure S8 Model-fitting and testing of an anti-sense oligonucleotide shift method of adapter concentration. **A** Fluorescence of the αL5 oligonucleotide in the staple-αL5-αL3 complex as a function of staple oligonucleotide quantity. Signal fits to a linear model (solid line). **B** Fluorescence of the αL3 oligonucleotide in the same complexes as A. Signal is again highly linear (solid line is a linear fit). **C** Known concentrations of L5 and L3 adapters and staple oligonucleotide were shifted by αL5 and αL3 and a fit to a linear model. As with staple oligonucleotides, data is linear: the solid line represents a perfect fit, dashed lines represent + or – 3 fmols. **D** Error in the estimates made in panel C. The method is reasonably accurate, with average errors around 20%. The parameters (slope and intercept) from panel C were then used to estimate oligonucleotide concentrations for ligation efficiency determinations, after applying a scaling factor based on the fluorescence of αL5/ αL3 oligonucleotides in 50

152 fmol staple complexes. The calculation is described in github.com/dfporter/easyCLIP/doc/ in
153 the README_fluorescence.md file.
154
155 **Figure S9** Quantification of cross-link rates for endogenous hnRNP C by immunoblot shift.
156 Cells were UV cross-linked cells then hnRNP C was immunopurified. The change in western
157 blot signal corresponding to monomeric hnRNP C was compared between RNAse
158 concentrations (panels A-C). Because this change in signal is specifically for what can be
159 collapsed with RNAse to monomeric hnRNP C, not for the un-collapsible higher molecular
160 weight complexes spread throughout the lane, it should agree with the cross-linking number
161 derived from dividing the RNA quantified in the minimal region by the monomeric hnRNP C
162 signal (Figure 4C) and be lower than that derived from all RNA across the gel. **A** RNAse
163 digestion series of immunopurified hnRNP C (immunoblot, anti-hnRNP C). **B** Example
164 replicate of +/- RNAse gels used to quantify the amount of shifted hnRNP C. **C** Quantification
165 of the amount of shifted immunoblot signal comparing +/- RNAse gel lanes, as in panel B.
166 The change in western blot signal was ~20%, close to the 22% cross-link number from Figure
167 4C. A more exact comparison was then performed, deriving the amount of hnRNP C protein
168 dependent on both UV cross-linking and RNAse-digestion by absolute quantification of a
169 western blot (panels D-F). **D** Gel used for absolute quantification of UV- and RNAse-
170 depending monomeric hnRNP C signal. **E** Standards used for absolute quantification of gel
171 data as in panel D. **F** Quantification of the absolute amount of protein present in the bands in
172 replicates like that in panel D. **G** The amount of hnRNP C cross-linked to RNA that is
173 collapsible into the monomeric hnRNP C band, as determined by the absolute quantification
174 data in panel F. This method also gave a cross-link rate of ~20%, again similar to the 22%
175 observed in Figure 4C. It was concluded that this method of determining cross-link rates
176 using absolute quantification of RNA and protein (Figures 2 and 3) was reasonably accurate.
177 This verification was only possible for hnRNP C because of its very high cross-link rate and
178 small size.
179
180
181 **Figure S10 A** Purification of randomly selected HA-tagged non-RBPs. Red represents L5
182 adapter fluorescence, and green anti-HA immunoblotting. **B** Total purified cross-linked RNA
183 positively correlates with protein size for randomly selected non-RBPs. **C** Immunoblot and
184 RNA visualization of the two non-RBPs that purified the most cross-linked RNA, UBA2 and
185 EPB41L5, shows cross-linked bands running a little higher than the minimal region. **D** Read
186 counts (per million reads) of the non-RBPs *vs* their own RNAs shows each non-RBP enriches
187 for its respective RNA, a consequence of each non-RBP being expressed from a plasmid.
188 This shows each library was generated from cells over-expressing the respective protein-of-
189 interest, despite the fact that barcodes for multiple over-expression experiments were
190 combined after each ligation. It also shows that if you express an RNA highly, it will show up
191 in CLIP data, regardless of the purified protein. Counts were capped at 5,000 reads-per-
192 million for visualization. Libraries for CAPNS6 were extremely small and were not included.
193 **E** Distribution of reads between introns and exons in mRNA for randomly selected non-RBPs.
194
195 **Figure S11** Expression levels of FH-PCBP1 and mutants in HCT116 cell lysate. The nature
196 of the additional, higher molecular weight bands (b, c) is unknown.
197

198 **Figure S12** Microscopy of wild-type and mutant FHH-PCBP1 in HCT116 cells showing that
199 L100P/Q mutants are less nuclear than wild-type or ΔKH2 PCBP1. All images were taken
200 with the same settings (exposure time, *ect.*), on the same slide and day.
201

202 **Supplementary Methods**

203 *L5 linker labelling*

204 0.5 mg IRDye 680RD DBCO (LI-COR, 429 nmol) was resuspended in 42.9 µL PBS for a
205 concentration of 10 mM. The L5 linkers (Azide-DNA-RNA oligonucleotides) were ordered
206 from IDT and resuspended in PBS. Oligonucleotides were run through a Zymo RNA-
207 clean-and-concentrator kit (purification was required for labelling), using ~14 µg
208 oligonucleotide per column and eluting at ~1 mg/mL (~85 µM) in water. 5 µL of 10 mM
209 dye (~50 nmol) was added to 10-150 µg purified oligonucleotide (~1-12 nmol) in PBS for
210 a total volume of 200 µL and reacted for 2 hours at 37°. Oligonucleotides were then run
211 again through a Zymo clean-up kit and eluted in water. During column purifications,
212 washes were performed using an 85% ethanol in water solution made fresh each time, in
213 place of the kit's wash buffer. Concentrations were determined by A260 ratio using an
214 approximate ε=368,050 M^{-1}. Oligonucleotides were diluted to 10 nM in ligation buffer (50
215 mM Tris pH 7.5, 10 mM $MgCl_2$, 16.7% PEG400), 1 µL was blotted onto a nylon
216 membrane, and fluorescence was measured in an Odyssey CLx machine (LI-COR). This
217 was typically ~15,000 fluorescence units per fmol for full labelling.
218

219 *AAVS1 microscopy of PCBP1 integrants*

220 4-well plastic chamber slides (Lab-Tek Permanox, Sigma #C6932-1PAK) were coated
221 with 0.01% poly-L-lysine (Sigma #P4707) for 15 minutes, then washed twice with PBS,
222 left dry for 5-30 minutes, and then either stored under PBS or used immediately. HCT116
223 cells were plated at <20% confluency and grown at least 24 hours before staining. Cells
224 were washed 1-2 times with PBS, then fixed for 10 minutes in 4% formaldehyde (in PBS)
225 at room temperature, rinsed three times with PBS, and then permeabilized with PBS
226 containing 0.5% Triton X-100 and 10% goat serum. After permeabilization, cells were
227 stained for 1 hour at room temperature with the primary antibody at 1:200 dilution in PBS
228 containing 0.05% Triton X-100 and 1% goat serum. After staining, cells were washed
229 three times with PBS containing 0.05% Triton X-100, then 2-3 times in PBS without
230 detergent, and the slide chamber removed. After letting the cells dry for a few minutes,
231 one drop of DAPI mounting solution was added to each well and a coverslip was added
232 and sealed with acetone.
233

234 *AAVS1 integration*

235 ~2 µg repair template and ~1 µg Cas9/guide RNA plasmid were transfected using
236 lipofectamine into 6-well plates containing ~300,000 cells each. Two days later,
237 puromycin was added to 1 µg/mL and selection continued for at least 10 total days. To
238 determine expression levels, 10 µg to 80 µg of clarified lysate in 1-8 µL of CLIP lysis buffer
239 (typically 4 µL) was combined with 16 µL 1.6X LB (NuPAGE) and run on an SDS-PAGE
240 gel. hnRNP C was immunoblotted using labelled anti-hnRNP C antibody (Santa Cruz,
241 798-conjugated) at 3 µL in 5-7 mL PBS blocking buffer (Licor), incubating for 30 minutes
242 and washing with PBS for 20 minutes. To immunoblot for the HA tag, ~3 µL Rabbit anti-
243 HA (COVANCE) in 5-7 mL blocking buffer, followed by ~3 µL IR680 or IR800 labeled
244 Goat anti-Rabbit (Licor) in 5-7 ml were used.
245

246 *AAVS1 integrated FHH-tagged protein purification*

15 µL anti-HA magnetic beads and 2-4 mg clarified lysate were used per immunopurification. Immunopurifications were carried out at 4° for 1 hour in 1 mL of CLIP lysis buffer.

GST-tagged protein constructs

pGEX-6P-1 vector was digested with BamHI and CSRP2-FLAG-HA was cloned in using In-Fusion (Takara). Amplification primers for CSRP2-FLAG-HA were:

Left primer	GGGGCCCCTGGGATCCATG CCGAACTGGGGAG
Right primer	GATGCGGCCGCTCGAGTCATGAACCTGCAGCATAGTCAGGCACATC

The GST moiety (and protease site) is 231 amino acids (26.8 kDa), and CSRP2-FLAG-HA is 217 amino acids (23.2 kDa), for a 448 amino acid (50 kDa) construct. This resulting sequence is given below, with CSRP2-FLAG-HA underlined (* denotes stop):

MSPILGYWKIKGLVQPTRLLLEYLEEKYEEHLYERDEGDKWRNKKFELGLEFPNLPYYI
DGDVKLTQSMAIIRYIADKHNMLGGCPKERAEISMLEGAVLDIRYGVSRIAYSKDFETLK
VDFLSKLPEMLKMFEDRLCHKTYLNGDHVTHPDFMLYDALDVVLYMDPMCLDAFPKL
VCFKKRIEAIPQIDKYLKSSKYIAWPLQGWQATFGGGDHPPKSDLEVLFQGPLGSMPN
WGGGKKCGVCQKTVYFAEEVQCEGNSFHKSCFLCMVCKKNLDSTTVAVHGEEIYCK
SCYGKKYGPKGYGYGQGAGTLSTDKGESLGIKHEEAPGHRPTTNPNASKFAQKIGGS
ERCPRCSQAVYAAEKVIGAGKSWHKACFRCAKCGKGLESTTLADKDGEIYCKGCYAK
NFGPKGFGFGQGAGALVHSELEDYKDDDDKAGYPYDVPDYAAGS*

The GST-hnRNP C construct (54 kDa) was cloned into the same site but did not include HA or FLAG tags. The resulting sequence is below:

MSPILGYWKIKGLVQPTRLLLEYLEEKYEEHLYERDEGDKWRNKKFELGLEFPNLPYYI
DGDVKLTQSMAIIRYIADKHNMLGGCPKERAEISMLEGAVLDIRYGVSRIAYSKDFETLK
VDFLSKLPEMLKMFEDRLCHKTYLNGDHVTHPDFMLYDALDVVLYMDPMCLDAFPKL
VCFKKRIEAIPQIDKYLKSSKYIAWPLQGWQATFGGGDHPPKSDLEVLFQGPLGSMAS
NVTNKTDPRSMNSRVFIGNLNTLVVKKSDVEAIFSKYGKIVGCSVHKGFAFVQYVNER
NARAAVAGEDGRMIAGQVLDINLAAEPKVNRGKAGVKRSAAEMYGSVTEHPSPSPLL
SSSFDLDYDFQRDYYDRMYSYPARVPPPPPIARAVVPSKRQRVSGNTSRRGKSGFNS
KSGQRGSSKSGKLKGDDLQAIKKELTQIKQKVDSLLENLEKIEKEQSKQAVEMKNDKS
EEEQSSSSVKKDETNVKMESEGGADDSAEEGDLLDDDDNEDRGDDQLELIKDDEKEA
EEGEDDRDSANGEDDS*

GST-tagged protein purification

E. coli BL21 cultures transformed with pGEX-6P-1 were grown in 500 mL at 37° until OD600 ~0.8, at which time Isopropyl-1-thio-β-D-galactopyranoside (IPTG) was added to a final concentration of 0.5 mM, and cultures were grown for another ~1.5 h before harvesting. Cells were harvested by the method of S. Harper *et al.*[2], namely centrifuging at 4,000 rcf for 20 min at 4°, resuspending in ~50 mL LB, and centrifuging again at 4,000

289 rcf for 20 min at 4°. Cell pellets were frozen in dry ice until purification. When thawed, the
290 cell pellet was resuspended in 20 mL of lysis buffer (50 mM Tris, 10 mM β–
291 mercaptoethanol, 50 mM NaCl, 5 mM EDTA, 1% Triton X-100, Roche protease inhibitor,
292 5% glycerol). Lysozyme was added very approximately to ~1 mg/ml, froze the pellet again
293 in dry ice, thawed in a water bath, and lyzed by sonication. The lysate was clarified by
294 centrifugation at ~21,000 rcf, 4°, for 15 min. 4 mL of 50% glutathione-agarose (Pierce)
295 was washed with resin wash buffer (Dulbecco PBS with 10 mM β–mercaptoethanol), and
296 then incubated at 4° in a 50 mL Falcon tube with clarified lysate for ~30 min before loading
297 on a column. The column was washed with 50 mL of 4° wash buffer (Dulbecco PBS with
298 10 mM β–mercaptoethanol, 5% glycerol and Roche protease inhibitor). Samples were
299 eluted in batch with three incubations at 4° with 1.5-2 mL elution buffer (100 mM Tris pH
300 8.0, 150 mM NaCl, 10 mM β–mercaptoethanol, 5% glycerol, 10 mM glutathione).
301
302 *GST-tagged protein quantification*
303 Following the method of K. Janes[3], BSA standards were run on a gel at 10, 5, 2.5, 1.3,
304 0.6, 0.3, and 0.15 µg, along with purified protein. Following the method of S. Luo *et al.*[4],
305 gels were washed for 10 minutes in water, stained for 10 minutes with staining buffer
306 (50% methanol, 10% acetic acid, 0.02% Coomaisse R250) at room temperature, followed
307 by destaining for 10 minutes with destaining buffer (40% methanol, 7% acetic acid), and
308 washing twice for 10 minutes with water. A third wash was performed overnight. Protein
309 was then visualized by scanning the 700 nm channel on a Licor Odyssey scanner. A
310 hyperbolic curve of band fluorescence *vs* input protein weight was fit to BSA standards.
311 Specifically, the parameters 'a' and 'b' in the equation y = a*x/(b+x), where 'x' is protein
312 weight and 'y' is fluorescence, were fit using least-squares regression. This curve was
313 used to determine the concentration of purified protein.
314
315 *Western blot protein quantification*
316 Following the method of K. Janes[3], purified GST-tagged protein standards were run
317 alongside the samples to be quantified. Purified GST-hnRNPC2 and purchased FBL
318 (Prospec, cat. enz-566) were diluted in protein dilution buffer (0.5X PBS, 0-5% glycerol,
319 0.05% Tween-20, 0.2 mg/mL BSA) to 20 ng/µL. Two-fold dilutions down from 20-100
320 ng/µL were made for a total of 8 concentrations; this solution was then delivered as 14
321 µL aliquots to multiple striptube aliquots and frozen at -80°. When running gels, 10 µL
322 from each concentration were combined with 10 µL loading buffer (3.6X NuPAGE loading
323 buffer with 10% β-mercaptoethanol), heated at 75° for 15 minutes, and loaded on a 4-
324 12% NuPAGE gel. Standards were therefore present at ~1000-3 ng per lane.
325 Immunoblotting against the HA epitope was performed with 1:3000 αHA conjugated to
326 Alexa Fluor 488 and incubating for 1 hour at room temperature in PBS blocking buffer (LI-
327 COR); images were taken in a GE Typhoon scanner (532 nm laser, 526SP filter, 500
328 PMT, 200 µm resolution). When small aliquots of immunopurification beads were loaded
329 on a gel, BSA was first added to 0.2 mg/mL to prevent absorption.
330
331 *BCA*
332 For BSA standards, 105 µL PBS was combined with 20 µL BSA (2 mg/mL stock) and 3
333 µL lysis buffer for the highest concentration of BSA, and 115 µL PBS, 10 µL BSA, and 3
334 µL lysis buffer for the second highest concentration. For lysate samples, 3 µL lysate was

335 combined with 125 µL PBS. For both standards and samples, serial dilutions were made
336 by a factor of three into PBS with 0.024% lysis buffer. Duplicate wells were used for each
337 sample. 25 µL of each well was transferred to a second 96-well plate and combined with
338 200 µL working reagent (Pierce BCA kit, 50:1 A:B). Plate was incubated for 20-30 minutes
339 at 37°. Absorbance was measured at 562 nm.
340
341 *Creation of cross-linked hnRNP C standard.*
342 Four replicates of 906-1600 µg of HCT116 lysate from cross-linked cells was added to
343 ~20 µL Protein G Dynabeads (ThermoFisher Cat #10003D) coupled with 25 µL (5 µg)
344 anti-hnRNP C (4F4) antibody per replicate. Immunoprecipitation was carried out at 4° for
345 ~1 hour, followed by the standard easyCLIP protocol for cross-link rate determination.
346 The RNAse digestion was performed with half of the samples treated with 0.1 U/µL
347 RNAse ONE for 10 minutes, and the other half of the samples treated with 0.05 U/µL
348 RNAse ONE for ~5 minutes. The PNK reaction was 14 minutes at 37°. The ligation was
349 performed overnight (17 hours) with 20 pmol L5 (barcode 23), and 2 µL high concentration
350 T4 RNA ligase (NEB). Samples were combined, and ~20 aliquots comprising 2.5% of the
351 beads (~10 ng hnRNP C each, ~400 ng total purified) in ~15 µL 1.6X NuPAGE buffer
352 were frozen in dry ice and kept long term at -80°. Immunoblotting was performed with
353 ~1:3000 αhnRNP C conjugated to AF790 (Santa Cruz Biotechnology, sc-32308 AF790),
354 which is visible on the 800 nm channel in a LI-COR Odyssey scanner, in PBS blocking
355 buffer (LI-COR) for ~1 hour at room temperature.
356
357 *Sequencing library creation: hnRNP C and FBL.*
358 HEK293T cells were grown to 30-90% confluency in petri dishes in DMEM with 10% Fetal
359 Bovine Serum, media was removed by vacuum, cells were washed with 4° PBS, and UV
360 cross-linked (254 nm) in 10 cm or 15 cm plates in a Stratalinker at 0.3 J/cm^2. After cross-
361 linking, 1 mL 4° lysis buffer (15 cm plates) or 0.5 mL lysis buffer (10 cm plates) was added
362 to each plate, cells were harvested with a rubber spatula and frozen in dry ice. CLIP lysis
363 buffer was as in Zarnegar *et al.*[5], except the concentration of Triton X-100 was 1% (see
364 File S1 for all buffers used for CLIP). For each hnRNP C replicate, 4 µg hnRNP C1/C2
365 Antibody (4F4, Santa Cruz Biochnology #sc-32308) and 20 µL Dynabeads Protein G for
366 Immunoprecipitation (ThermoFisher, #10003D) were coupled for 1 hour at room
367 temperature before adding 600 µg of clarified HEK293T lysate and immunopurifying at 4°
368 for 45-60 minutes. For FBF, two replicates of 4 mg clarified lysate were combined with 20
369 µL Fibrillarin Antibody (Bethyl, #A303-891A) and 20 µL Protein G Dynabeads;
370 immunopurification was at 4° for 1 hour. The easyCLIP assay was performed as
371 described in File S1.
372
373 *easyCLIP: library creation.*
374 The full easyCLIP protocol and all buffers are described in File S1. After harvesting, cells
375 were thawed and lyzed with a microtip sonicator six times for five seconds each (10%
376 power), with samples cooled by placement in dry ice between sonications. Lysates were
377 then clarified by spinning at 14 krcf for 10 minutes at 4° and transferring the supernatant
378 to a new tube. Concentrations were determined by BCA (see BCA section). To visualize
379 protein expression levels, 15 µg of clarified lysates were used for western blotting. For
380 immunopurification, typically 20 µL of anti-HA beads per sample were washed with NT2

381 buffer, then CLIP lysis buffer. Samples were diluted to 1-4 mg/mL during
382 immunopurification, typically ~2 mg/ml. Immunopurification was 40 minutes to 1 hour at
383 4°. Samples were then washed once with H. Str. Buffer (10 minutes), H. Salt buffer (10
384 minutes), low salt buffer, and finally NT2 buffer, each with 1 mL. Samples were then
385 stepped down with another wash to ~200 µL NT2 buffer. RNAse digestion was performed
386 by diluting 2 µL 100 U/µL RNAse ONE to 1 U/µL in NT2 buffer, then diluting this to 0.025
387 U/µL in NT2 buffer with 16% PEG and adding 60 µL of this to each sample. The digestion
388 was performed for 8-12 minutes at 30° with intermittent shaking. The digestion mixture
389 was removed from the beads and 1 mL H. Str. Buffer was added. Samples were then
390 washed twice with 1 mL NT2 buffer before being stepped down to ~200 µL NT2 buffer.
391 Samples were then processed in the order (1) kinase, (2) 5' ligation, (3) L5 barcodes
392 combined, (4) phosphatase, (5) 3' ligation, or in the order (1) phosphatase, (2) 3' ligation,
393 (3) L3 barcodes combined, (4) kinase, (5) 5' ligation. Processing details and
394 oligonucleotide sequences are in File S1. In either case, all samples were typically
395 combined before being loaded into a single lane of a 4-12% NuPAGE Bis-Tris gel, run at
396 200V for ~45 minutes, and transferred to nitrocellulose at 400-500 mA for ~25 minutes.
397 Membranes were then placed in PBS and immediately imaged in an Odyssey CLx
398 machine. Membranes were cut using scalpels and put in 375 µL PK buffer with 25 µL
399 Proteinase K and incubated for 40-60 minutes with shaking at 45-55°. In some cases, 2
400 µL of extracted RNA was then spotted on nylon and imaged. PK mixtures were added
401 directly to 20 µL oligonucleotide(dT) beads and mixed at room temperature for 20
402 minutes. Alternatively, 2 M KCl was added and SDS was spun out, then 20 µL
403 oligonucleotide(dT) beads were added and the samples were mixed at 4° for 20 minutes.
404 Beads were washed once with biotin IP buffer, once with NT2 buffer, transferred to a PCR
405 tube, then washed 3-4 times with PBS buffer. Samples were eluted in 14.4 water with 15
406 pmol reverse transcription primer by heating at 95° for 3 minutes and transferring to a
407 new tube. Reverse transcription was performed by incubating for 40 minutes at 53° and
408 10 minutes at 55°, or in some cases for 40 minutes at 53° only. Reverse transcription
409 product was then used directly for PCR as described in File S1.
410
411 *Ligation efficiency test by protein shift.*
412 The ligation efficiency test with hnRNP C was performed in three replicates. hnRNP C
413 was purified by incubating 600 µg of clarified HEK293T lysate with 4 µg anti-hnRNP
414 C1/C2 antibody for 1.5 hours at 4° as described previously[5]. Beads were RNAse digested
415 and dephosphorylated as described previously, before being split 2:1. The split
416 corresponding to 200 µg lysate was PNK phosphorylated and 5' ligated as described in
417 the easyCLIP protocol. The split corresponding to 400 µg was 3' ligated as described
418 previously, before being split in half. One 3' ligated split was PNK phosphorylated and 5'
419 ligated as described in the easyCLIP protocol. All samples were then run on a 4-12%
420 SDS-PAGE gel (NuPAGE), transferred to nitrocellulose and visualized as described
421 previously. The amount of RNA that was neither 5' nor 3' ligated was determined by the
422 following reasoning. First, let P5 be the probability of a 5' ligation, and P3 be the
423 probability of a 3' ligation. Let a = RNA with no ligation; b = RNA with a 3' ligation only; c

= RNA with a 5' ligation only; and d = RNA with a 5' and 3' ligation. Let T = the total amount of RNA. It follows that:

$$b * c = (T * P3(1 - P5)) * (T * P5(1 - P3))$$
$$a * d = (T * (1 - P5)(1 - P3)) * (T * P5P3)$$

Rearranging terms shows that a*d = b*c. Since d, b, and c are determined by direct visualization of fluorescence, it follows that the RNA with no ligation (a) is also known.

Fluorescence loss

20 µL of Streptavidin Dynabeads (ThermoFisher) per purification were washed three times with BIB, then combined with 2 µL of 5 µM biotin-anti-L5 RNA (10 pmol, ordered as /5BiosG/rUrArCrCrCrUrUrCrGrCrUrUrCrArCrArCrArCrArCrArArG from IDT, with an RNAse free HPLC purification). The oligonucleotide was captured for 20 minutes in 1 mL BIB, then washed with BIB, NT2, PBS (1X each) and resuspended in 50 µL BIB.

6.4 µL 2 M KCl was added to proteinase K-digested samples, and SDS was precipitated on ice for 15 minutes. SDS was spun out at 13 kRPM for 10 minutes. Dynabeads with 10 pmol biotin-anti-L5 RNA oligonucleotide in 50 µL BIB were then added to PK reactions and diluted to a total volume of 1 mL with BIB. The purification was carried out at 4° for 20 minutes. Beads were washed three times with BIB, twice with PBS, and eluted for 2 minutes at 95° in 15-20 µL water with 100 nM biotin.

10X NT2 was added to 1X final concentration, and PEG to 16% final concentration. 1 µL 100 U/µL RNAse ONE was added and samples incubated for 40 minutes at 37°. RNAse ONE was inactivated by adding 10% SDS to 0.1%. Shift buffer was added to 1X (25 mM Tris pH 7.5, 10 mM $MgCl_2$, and 16% PEG400). 300-400 fmol labelled antisense oligos were added and samples were processed further as described for the ligation efficiency test by anti-sense oligo shift.

Shift oligos:

αL5	/5AzideN/TACCCTTCGCTTCACACACACAAG	24 nt
αL3	/5AzideN/TTTTTCTGAACCGCTCTTCCGATCTCAG	28 nt

300-400 fmol labelled antisense oligonucleotides were added (max is ~500 fmol before signal cannot be quantified). The relative amount of shift oligonucleotide to input is important, as excessive oligonucleotide will create artifacts. Heat at 75° for 2 minutes, then let sample sit at room temperature for at least a minute. Create samples for two lanes of shift oligonucleotides at 300 fmol per lane (or however much was used to shift). Running the shift oligonucleotides at the same concentration used to shift is required to subtract background. Add 6X Ficoll/BPB buffer (15% Ficoll 400, 0.03% Bromophenol blue, 50 mM Tris pH 7.5) to 1X, but do not heat. For gel running buffer, add NaCl to 25 mM in 4° 0.5X TBE buffer. Samples were loaded on a 20% TBE gel and run gel 180V at 4° for one hour, replacing running buffer with 4° buffer every ~40 minutes. Finally, samples were transferred to nylon in 0.5X TBE buffer at 250 mA for 30 minutes.

466 *Ligation efficiency test by RNA shift.*
467 Samples of hnRNP C were prepared as normal for easyCLIP (File S1), and as described
468 for the protein shift ligation efficiency test, up to the proteinase K extraction from
469 nitrocellulose. To inactivate proteinase K, 6.4 µL 2M KCl per 400 µL of proteinase K
470 extract was added, samples incubated at 4° for 15 minutes, and precipitated SDS
471 removed by centrifugation at 13,000 RPM for 10 minutes at 4°.
472
473 Two sets of MyOne C1 Streptavidin beads were prepared, each using 13-20 µL MyOne
474 C1 streptavidin beads per sample: one set for biotin purification and one for antisense
475 oligonucleotide purification. Beads were washed three times with Biotin IP Buffer (BIB:
476 100 mM Tris pH 7.5, 1 M NaCl, 0.1% Tween-20, 1 mM EDTA). Those to be used for the
477 biotin purification were then set aside until use. The set for anti-sense oligonucleotide
478 purification were then incubated with 30 pmol anti-sense biotinylated oligonucleotide per
479 µL resin in 1 mL BIB and rotated for 20 minutes at room temperature. Solution was
480 removed and a second incubation with 15 pmol biotinylated oligonucleotide per µL resin
481 was performed to ensure saturation. After incubation, anti-sense oligonucleotide beads
482 were washed with BIB, NT2, PBS, and resuspended in 750 µL BIB. 50 µL of this bead
483 solution was added to 400 µL BIB containing 20 nmol biotin and mixed. This solution was
484 allowed to sit at room temperature for at least 5 minutes.
485
486 Proteinase K extract was bound to beads and incubated for 20 minutes at 4°. Supernatant
487 was removed and beads were resuspended in 200 µL BIB, transferred to a PCR tube,
488 rinsed with 200 µL NT2, washed with 200 µL PBS, and allowed to at least briefly reach
489 20-25°. After reaching room temperature, supernatant was removed and libraries eluted
490 in 18 µL formamide at 65° for 2 minutes.
491
492 *Ligation efficiency test by anti-sense oligonucleotide shift.*
493 Beads were washed three times with BIB, twice with PBS, and eluted for 2 minutes at 95°
494 in 15-20 µL water with 100 nM biotin. Add 10X NT2 to 1X, and PEG to 16% final
495 concentration. Add 1 µL 100 U/µL RNAse ONE. Incubate 40 minutes at 37°. Add 10%
496 SDS to 0.1% to inactivate RNAse ONE. Add shift buffer to 1X (25 mM Tris pH 7.5, 10 mM
497 $MgCl_2$, and 16% PEG400). Split the volume in three or four if doing separate shifts.
498
499 300-400 fmol labelled antisense oligos were added (max is 500 fmol before signal cannot
500 be quantified). The relative amount of shift oligo to input is important, as excessive oligo
501 will create artifacts. Samples were heated to 75° for 2 minutes, then cooled to room
502 temperature at -0.1°/s. 6X Ficoll/BPB buffer (15% Ficoll 400, 0.03% Bromophenol blue,
503 50 mM Tris pH 7.5) was added to 1X before loading on a gel. For gel running buffer, NaCl
504 to was added to 25 mM in 4° 0.5X TBE buffer. Samples were loaded on a 20% TBE gel
505 and run at 180V at 4° for ~1-3 hours, replacing running buffer with 4° buffer every ~40
506 minutes. Finally, samples were transferred to nylon in 0.5X TBE buffer at 250 mA for 30
507 minutes.
508
509 *Generation of linear cDNA standards*
510 Separately barcoded linear P3 and P6 fragments were ordered from IDT and stitched
511 together by oligo extension. P3 fragments were of the following form, with X indicating the

512 P3 barcode (Sequences in File 1). Fragments were mixed together in water and placed
513 at room temperature before running the stitching reaction. Fragments were stitched
514 together using Klenow fragment: 1 µL 100 µM of each oligo was combined with 10 µL
515 NEBuffer 3.1 (10X), 1.5 µL of 2 mM dNTPs and 1 µL Klenow Fragment (exo-), in 100 µL
516 reaction volumes. Reactions were incubated at 37° for 1 hour. 2 µL of Exonuclease I
517 (NEB) was added to each reaction and incubated at 37° for 1 hour. Samples were purified
518 with RNA clean and concentrator columns (Zymo) and eluted in 40 µL. Concentrations
519 were determined by the dsDNA Qbit assay, and 1 µL of each sample was run on a 15%
520 TBE-urea gel (NuPAGE). The dsDNA concentration obtained by Qbit was converted to a
521 molar quantity using a molecular weight and fluorescence per fmol was determined by
522 comparing the Qbit assay results and fluorescence on a TBE-urea gel. 3 fmol/µL samples
523 were run again on a gel to determine concentration, diluted to 80 amol/µL, adjusted based
524 on in-gel fluorescence, and finally diluted to 8 amol/µL. 0.3 µL of 8 amol/µL standards (2.4
525 amol) were added to CLIP PCR reactions. Consistency in final molar concentrations was
526 evaluated by qPCR and adjusted towards the average.
527
528 *CLIP analysis: genomes*
529 The GRCh38 genome Gencode release 29 and features were obtained from:
530 ftp://ftp.ebi.ac.uk/pub/databases/gencode/Gencode_human/release_29/GRCh38.primar
531 y_assembly.genome.fa.gz
532 ftp://ftp.ebi.ac.uk/pub/databases/gencode/Gencode_human/gencode.v29.primary_asse
533 mbly.annotation.gtf.gz.
534 The STAR index was built using --sjdbOverhang 75. When assigning reads to genes after
535 STAR mapping, only GTF features with transcript support level tsl1 or tslNA were
536 included.
537
538 For repetitive elements, an alignment file from was downloaded from
539 http://www.repeatmasker.org/. This was parsed to extract representatives, which were
540 placed in an artificial chromosome separated by poly(N), and a gtf file for each
541 representative was generated. A STAR index was built with --genomeSAindexNbases 5.
542 The parameter genomeSAindexNbases must be set well below the default of 14 or
543 building will be very slow. When mapping to the repeats chromosome, --alignIntronMax
544 1 was used to prevent the insertion of introns by STAR.
545
546 *CLIP analysis: read processing*
547 Custom Python scripts (github.com/dfporter/easyCLIP) were used for all analysis. Raw
548 fastq files were split by L5 and L3 barcodes allowing one nucleotide mismatches to the
549 expected barcodes. Reads were first mapped to a custom-built chromosome of repetitive
550 elements using STAR and "--alignEndsType EndToEnd". Unmapped reads from this
551 stage were then mapped to the regular genome using default parameters. Reads
552 mapping the genome to remove multimapping reads and MAPQ < 10 reads. Mapping
553 results from repetitive elements and the genome were combined, read mates removed,
554 results converted to BED format, and PCR duplicates removed using the random
555 hexamer UMI on the L5 adapter.
556

557 *CLIP analysis: read assignment*
558 Reads were assigned to an RNA if they overlapped only that RNA, or if they overlapped
559 a snoRNA element in any case. The strand was ignored for repetitive elements.
560
561 *CLIP analysis: statistics*
562 Inputs to statistical analysis were either reads per million or reads per ten billion proteins,
563 both treated the same. To speed up analysis, RNAs with a maximum count below five
564 (reads per million reads, or per ten billion proteins) across all samples were dropped from
565 all further analysis. For the randomly selected non-RBPs constituting background, if a
566 replicate had no reads it was assigned one tenth the minimum positive count present in
567 that dataset (i.e., if a dataset had one million reads, zeros were replaced with 0.1 reads
568 per million). The average count across replicates for each protein was determined,
569 resulting in a sample of eight values taken from the null distribution (one for each of the
570 proteins CDK4, CHMP3, DCTN6, ETS2, IDE, ITPA, TPGS2 and UBA2). σ^2/μ was
571 essentially always above 2 for these samples, and were fit to a negative binomial using
572 scipy[6] and calculated P values accordingly before finally adjusting all P values for each
573 protein by the Benjamini-Hochberg method into FDR equivalents.
574
575 *CLIP analysis: peak finding*
576 For each RNA, reads spanning the genomic locus were converted into an array with the
577 length of the genomic locus and each value representing the count of 5' read ends
578 mapping to that position. The values were smoothed by convolution using a box with
579 length 50 for loci of at least 2,000 nucleotides, length 20 for 20-2,000 nucleotides, and
580 length 10 for <200 nucleotides. If this array had a single maximum, it was taken to be the
581 peak location. If there were multiple maxima (equal heights) and no maxima had more
582 than a two nucleotide gap from another maxima, the peak was taken as the average
583 position between the first and last maxima. If any maximum was more than two
584 nucleotides from another maximum, the RNA was considered to have no peak.
585
586

587 **Supplementary references**

588 1. Van Nostrand, E. L. *et al.* Robust transcriptome-wide discovery of RNA-binding
589 protein binding sites with enhanced CLIP (eCLIP). *Nat. Methods* **13**, 508 (2016).
590 2. Harper, S. & Speicher, D. W. Purification of proteins fused to glutathione S-
591 transferase. *Methods Mol. Biol.* **681**, 259–280 (2011).
592 3. Janes, K. A. An analysis of critical factors for quantitative immunoblotting. *Sci.*
593 *Signal.* **8**, rs2 LP-rs2 (2015).
594 4. Luo, S., Wehr, N. B. & Levine, R. L. Quantitation of protein on gels and blots by
595 infrared fluorescence of Coomassie blue and Fast Green. *Anal. Biochem.* **350**,
596 233–238 (2006).
597 5. Zarnegar, B. J. *et al.* irCLIP platform for efficient characterization of protein—RNA
598 interactions. *Nat. Methods* **13**, 489–492 (2016).
599 6. Oliphant, T. E. Python for Scientific Computing. *Comput. Sci. Eng.* **9**, 10–20
600 (2007).
601

A

Fig S1

Method	Fraction of RT input to PCR	PCR cycles	fmols (σ)	fmols, extrapolated to 100% input to PCR (σ)	Fold increase	Fraction mappable	Minimum fold increase in mappable reads	Stated input library size, stated PCR efficiency	Input library size at 86% PCR efficiency	Input library size at 96% PCR efficiency
easyCLIP	16%	16	1,971 (241)	12,800 (1,445)	178	16%	30	NA	1,30,000,000 (2,100 amol)	226,000,000 (370 amol)
eCLIP	100%	16	72 (8)	72 (8)	1	Unknown, gel extracted	1	7,000,000 (12 amol), 86%	7,000,000 (12 amol)	NA

B

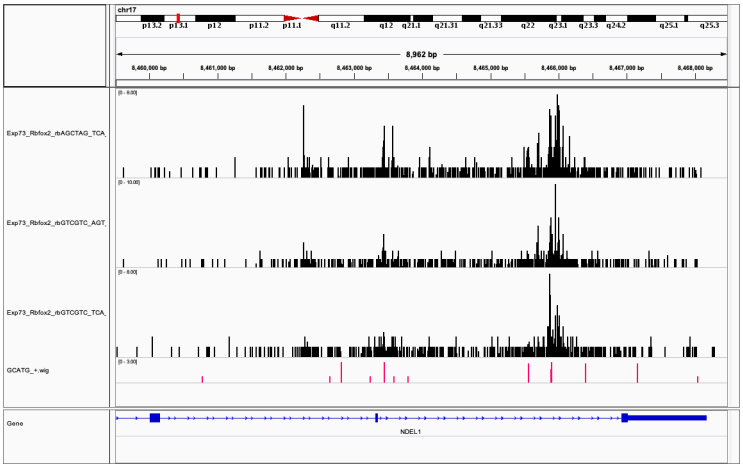

C

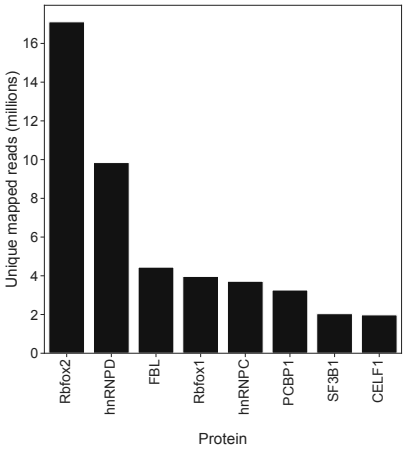

Fig S2

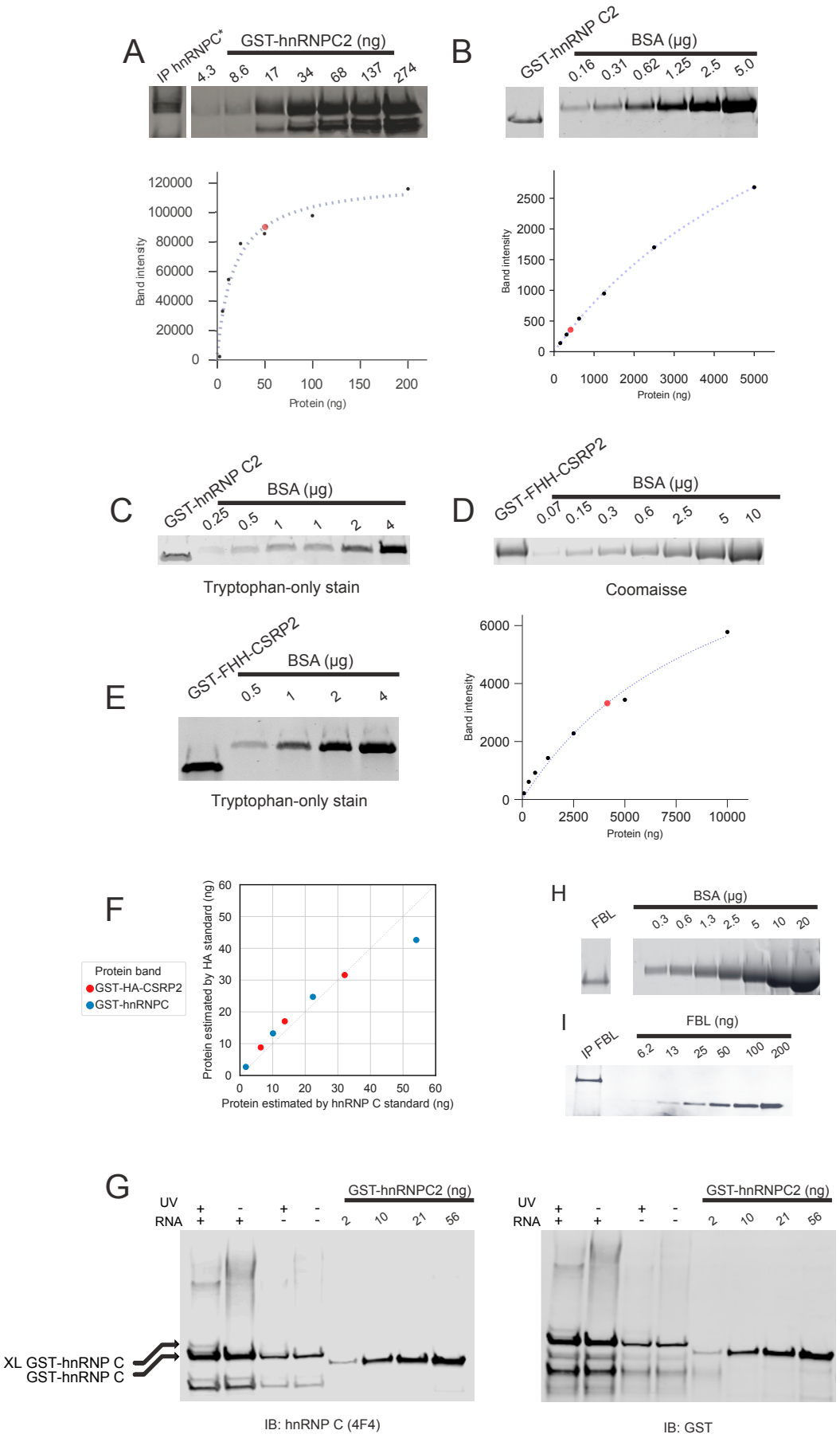
A
IP hnRNPC*
GST-hnRNPC2 (ng)
4.3
8.6
17
34
68
137
274
Band intensity
Protein (ng)
B
GST-hnRNP C2
BSA (µg)
0.16
0.31
0.62
1.25
2.5
5.0
Band intensity
Protein (ng)
C
GST-hnRNP C2
BSA (µg)
0.25
0.5
1
1
2
4
Tryptophan-only stain
D
GST-FHH-CSRP2
BSA (µg)
0.07
0.15
0.3
0.6
2.5
5
10
Coomaisse
E
GST-FHH-CSRP2
BSA (µg)
0.5
1
2
4
Tryptophan-only stain
Band intensity
Protein (ng)
F
Protein band
GST-HA-CSRP2
GST-hnRNPC
Protein estimated by HA standard (ng)
Protein estimated by hnRNP C standard (ng)
H
FBL
BSA (µg)
0.3
0.6
1.3
2.5
5
10
20
I
IP FBL
FBL (ng)
6.2
13
25
50
100
200
G
UV
RNA
GST-hnRNPC2 (ng)
2
10
21
56
XL GST-hnRNP C
GST-hnRNP C
IB: hnRNP C (4F4)
IB: GST

Fig S3

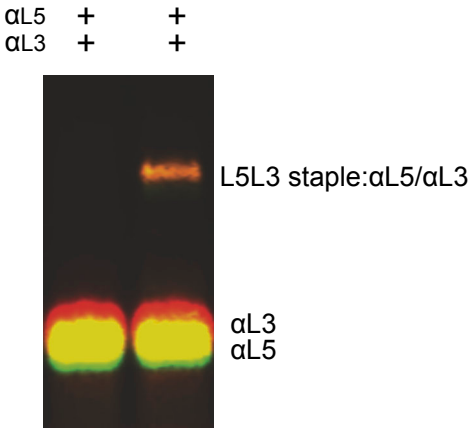

Fig S4

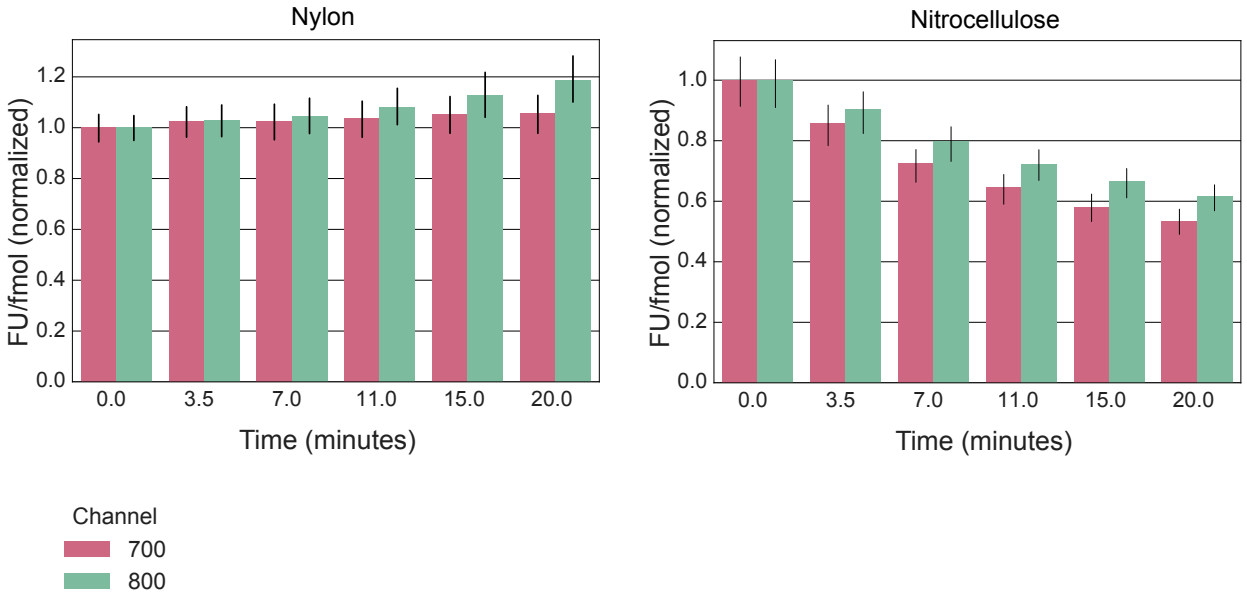
Nylon
Nitrocellulose
FU/fmol (normalized)
0.0
0.2
0.4
0.6
0.8
1.0
1.2
0.0
3.5
7.0
11.0
15.0
20.0
Time (minutes)
Channel
700
800

Fig S5

A

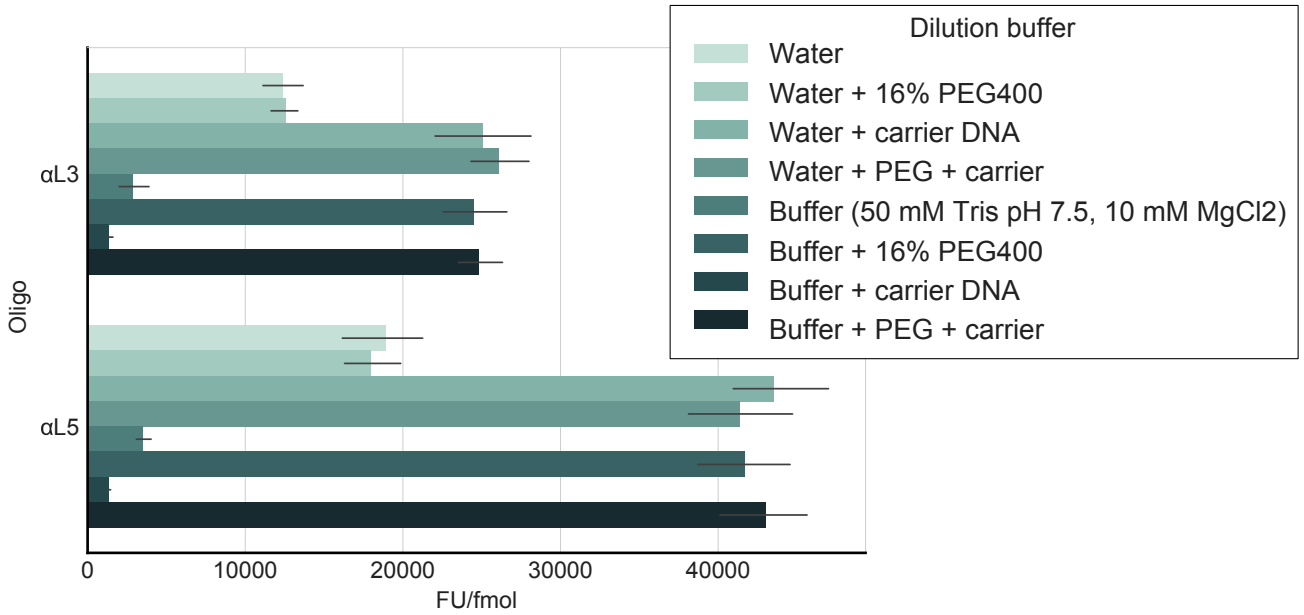

B

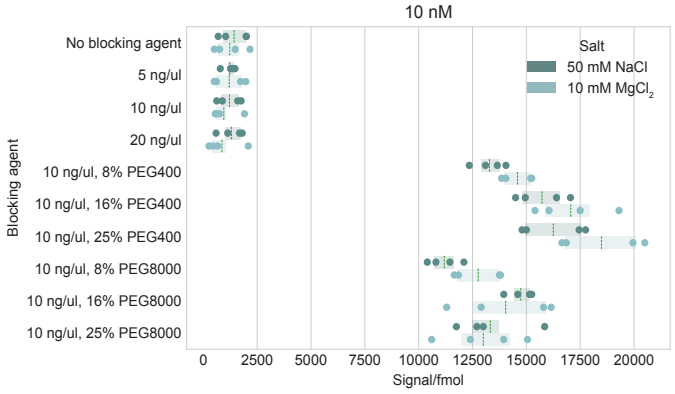

C

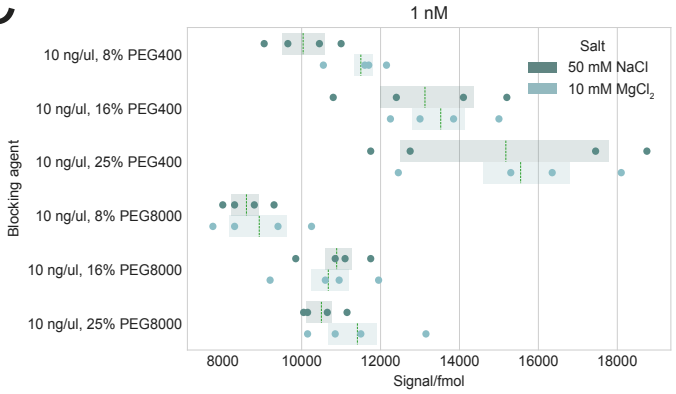

D

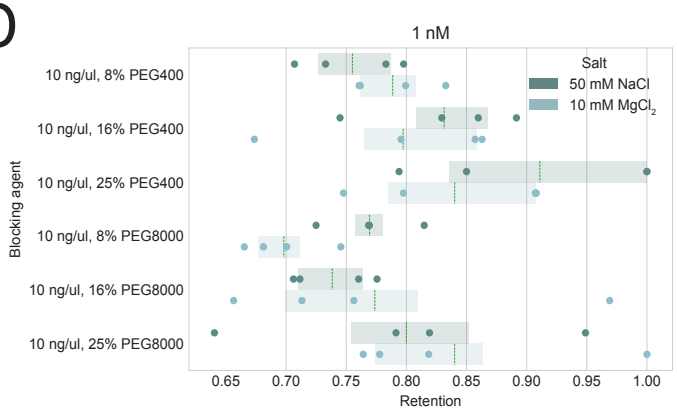

E

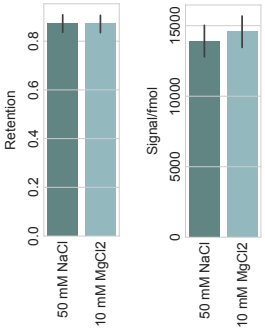

F

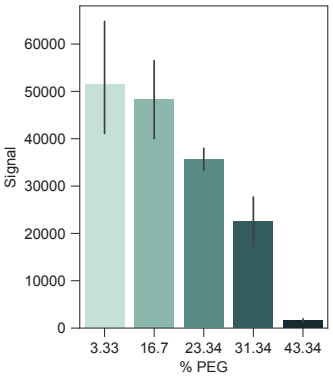

Fig S6

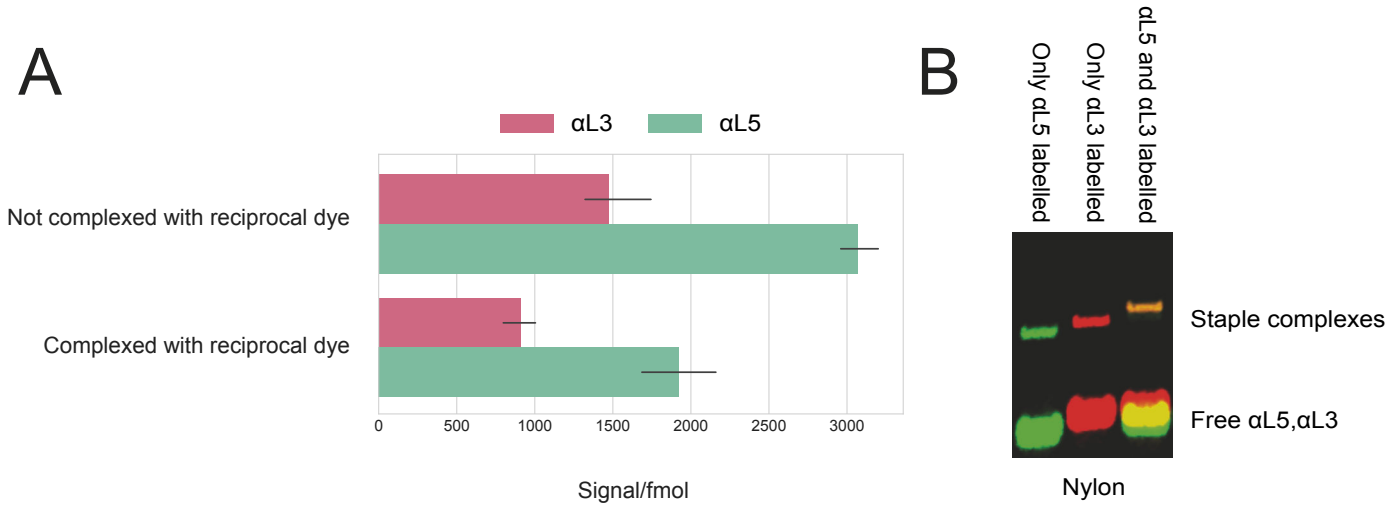
A
αL3
αL5
Not complexed with reciprocal dye
Complexed with reciprocal dye
0
500
1000
1500
2000
2500
3000
Signal/fmol
B
Only αL5 labelled
Only αL3 labelled
αL5 and αL3 labelled
Staple complexes
Free αL5,αL3
Nylon

Fig S7

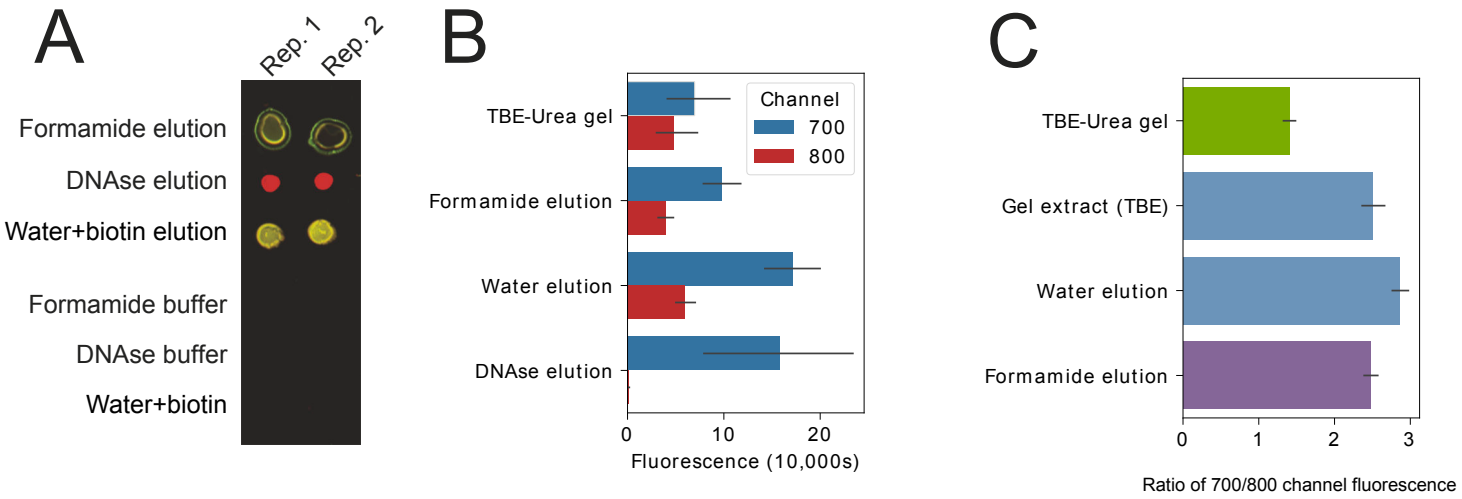
A
Rep. 1
Rep. 2
Formamide elution
DNAse elution
Water+biotin elution
Formamide buffer
DNAse buffer
Water+biotin
B
Channel
700
800
TBE-Urea gel
Formamide elution
Water elution
DNAse elution
0
10
20
Fluorescence (10,000s)
C
TBE-Urea gel
Gel extract (TBE)
Water elution
Formamide elution
0
1
2
3
Ratio of 700/800 channel fluorescence

Fig S8

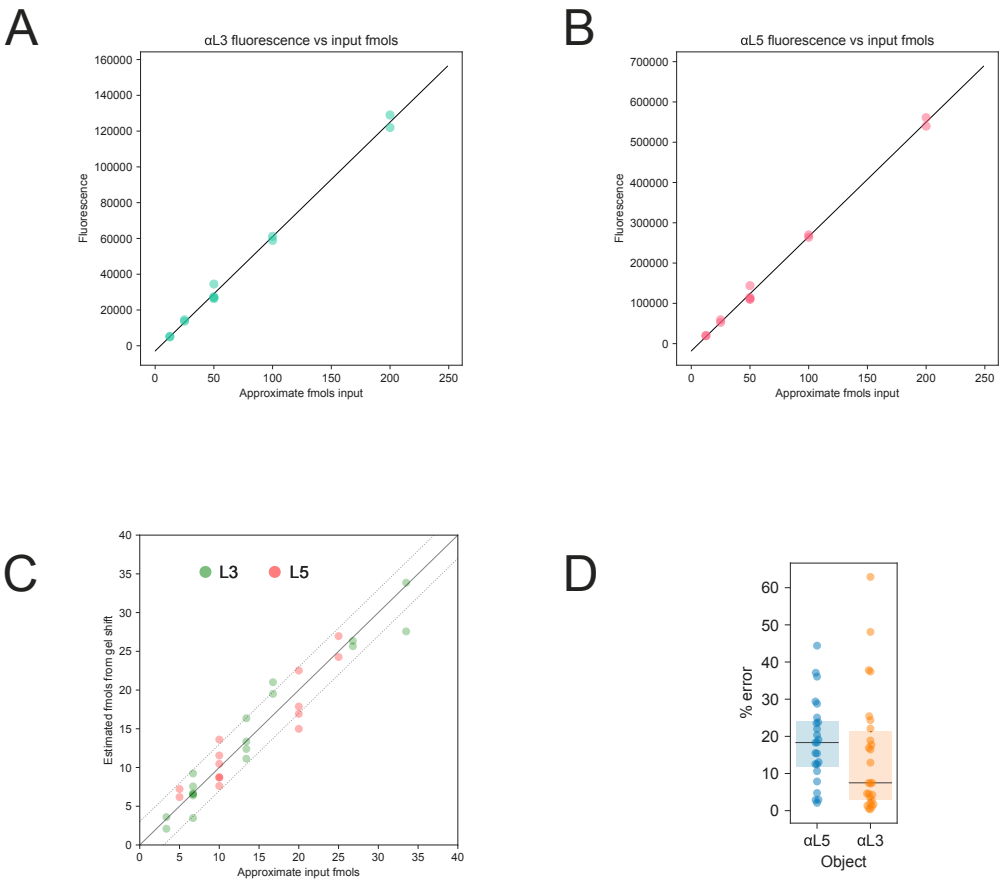
A
αL3 fluorescence vs input fmols
Fluorescence
Approximate fmols input
B
αL5 fluorescence vs input fmols
Fluorescence
Approximate fmols input
C
L3
L5
Estimated fmols from gel shift
Approximate input fmols
D
% error
αL5
αL3
Object

Fig S9

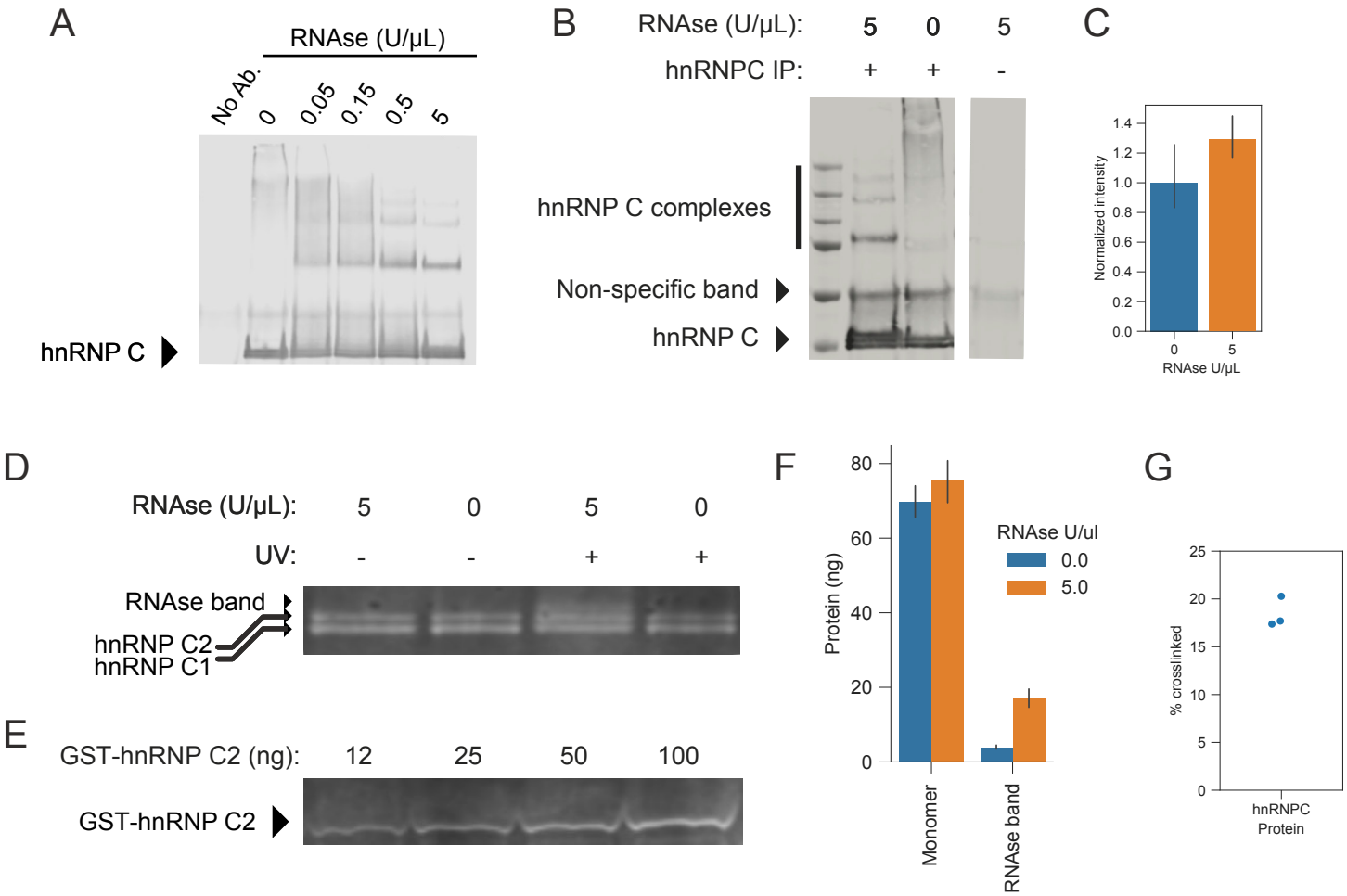
A
RNAse (U/μL)
No Ab.
0
0.05
0.15
0.5
5
hnRNP C
B
RNAse (U/μL): 5 0 5
hnRNPC IP: + + -
hnRNP C complexes
Non-specific band
hnRNP C
C
Normalized intensity
1.4
1.2
1.0
0.8
0.6
0.4
0.2
0.0
0
5
RNAse U/μL
D
RNAse (U/μL): 5 0 5 0
UV: - - + +
RNAse band
hnRNP C2
hnRNP C1
E
GST-hnRNP C2 (ng): 12 25 50 100
GST-hnRNP C2
F
Protein (ng)
80
60
40
20
0
RNAse U/ul
0.0
5.0
Monomer
RNAse band
G
% crosslinked
25
20
15
10
5
0
hnRNPC
Protein

Fig S10

non-RBPs usually purify little cross-linked RNA

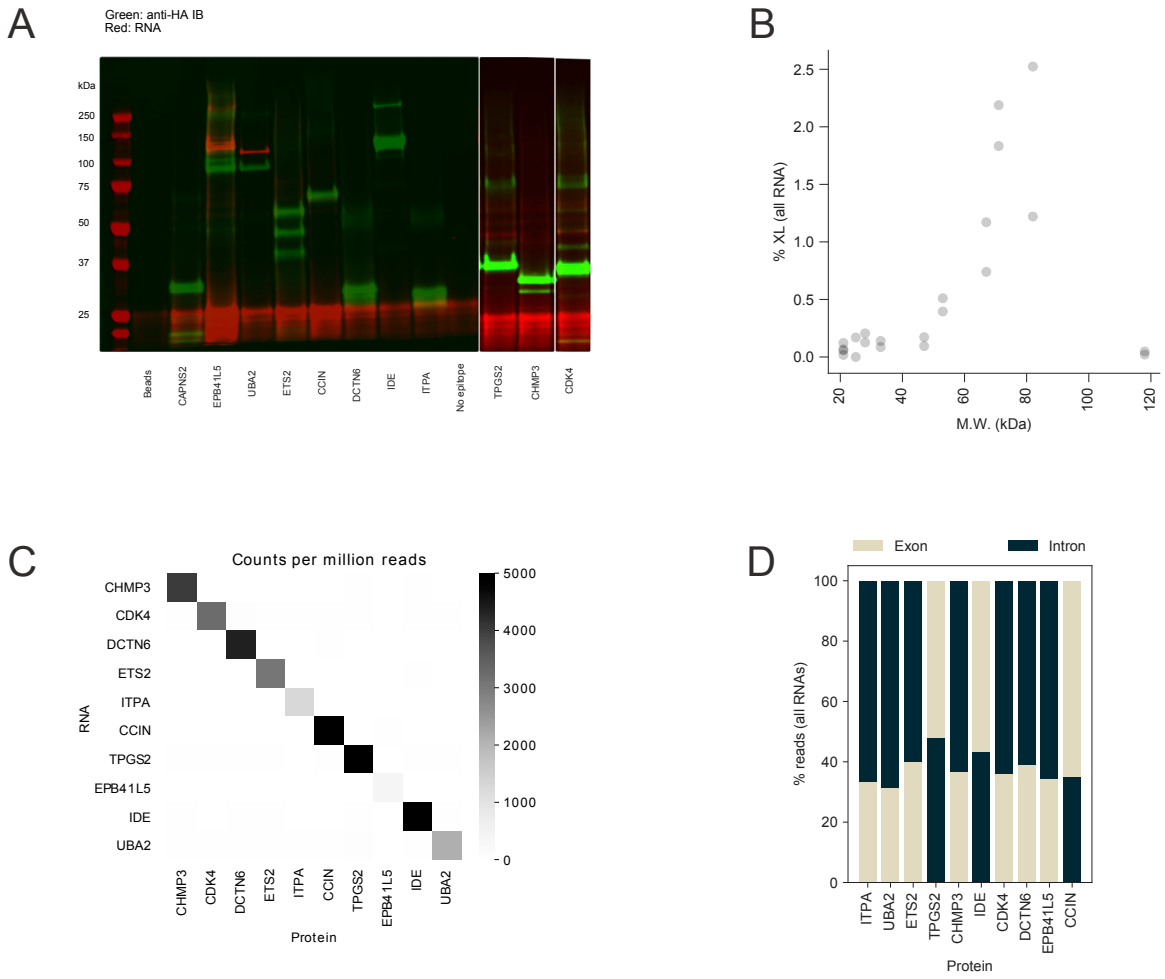

Fig S11

Expression levels of PCBP1 and mutants

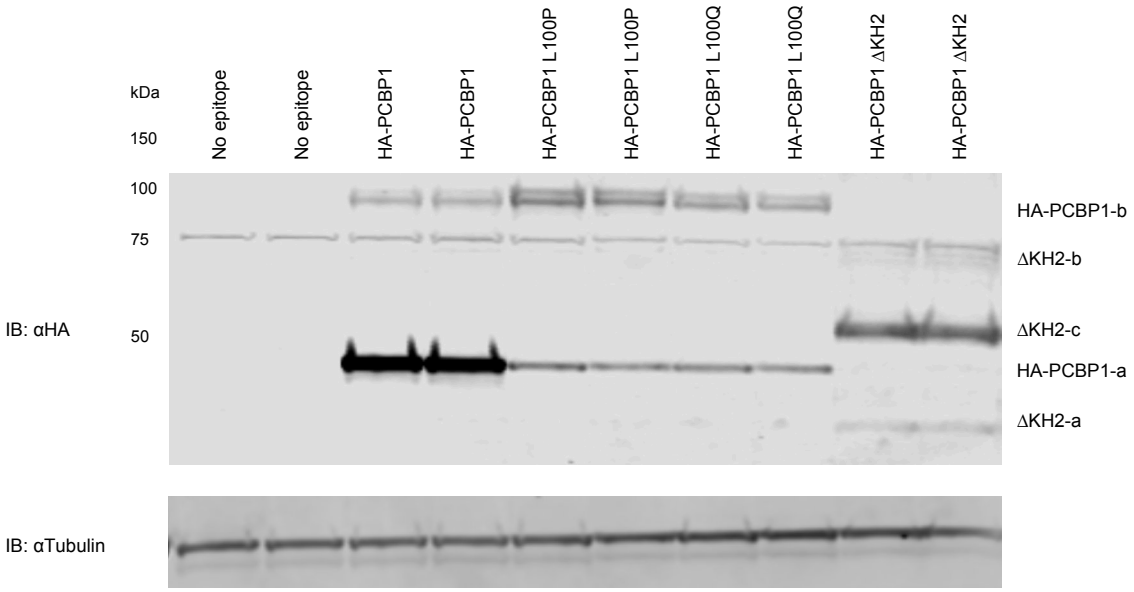

Fig S12

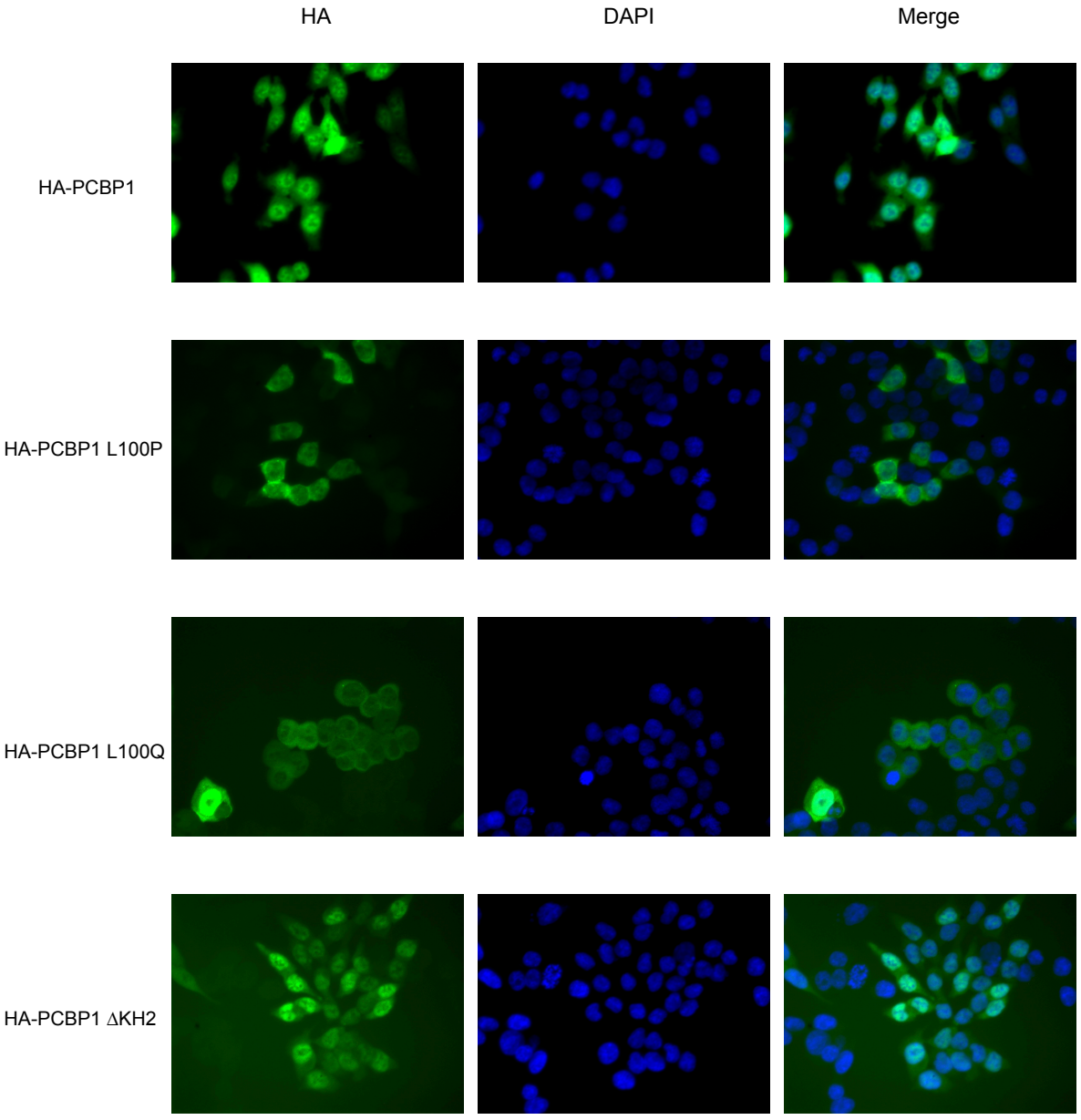
HA
DAPI
Merge
HA-PCBP1
HA-PCBP1 L100P
HA-PCBP1 L100Q
HA-PCBP1 ΔKH2